IMPROVEMENT OF FORECASTING APPROACHES BY USING WAVELET COHERENCE METHOD AND MULTIFRACTAL DETRENDED FLUCTUATION ANALYSIS

ITIR DOĞANGÜN

YEDITEPE UNIVERSITY
GRADUATE SCHOOL OF SOCIAL SCIENCES
İSTANBUL, 2023

IMPROVEMENT OF FORECASTING APPROACHES BY USING WAVELET COHERENCE METHOD AND MULTIFRACTAL DETRENDED FLUCTUATION ANALYSIS

BY

ITIR DOĞANGÜN

SUPERVISOR

PROF. ERKUT AKKARTAL

DISSERTATION SUBMITTED IN PARTIAL FULFILLMENT

OF THE REQUIREMENTS FOR THE DEGREE OF DOCTOR OF PHILOSOPHY

IN

DEPARTMENT OF FINANCIAL ECONOMICS

YEDİTEPE UNIVERSITY

JUNE, 2023

PLAGIARISM

I hereby declare that all information in this document has been obtained and presented in accordance with academic rules and ethical conduct. I also declare that, as required by these rules and conduct, I have fully cited and referenced all material and results that are not original to this work.

20.06.2023
ITIR DOĞANGÜN

ABSTRACT

This thesis comprehensively explores the multifractal structure characterizing precious metal prices and their dynamic relationships. Utilizing advanced techniques such as Vector Fractionally Integrated Autoregressive Moving Average (V-FARIMA) modeling and Multifractal Cross-Correlation Detrended Moving Average Analysis (MF-X-DMA), the research delivers critical insights into forecasting accuracy and risk-return tradeoff in commodities investments.

The initial portion of the research hones in on the multifractal structure inherent in precious metal prices, with a particular emphasis on periods of financial instability. The insights gathered in this phase contribute significantly to constructing precise predictions for commodity price variations, empowering investors to make knowledgeable decisions, manage risks effectively, and protect their investments even in a turbulent market.

The study then investigates the dynamic relationship between the return rates of gold and platinum, discovering substantial connections across varying frequencies and time frames. This finding supports the concept of co-movement behavior in commodities markets, further influencing risk management, portfolio diversification techniques, and the formation of effective trading strategies.

A notable discovery in this research is the consistent comovement over long periods of time as indicated by the constancy in Hölder exponents at lower frequencies. This result not only validates the proposed forecasting approach but also opens potential avenues for future investigations in the field.

The first section presents the effectiveness of the V-FARIMA model, emphasizing its superiority in forecasting the Hölder exponents of multifractal precious metal time series. The V-FARIMA model shows promise in spotting underlying trends and patterns in data, increasing our comprehension of price movements in precious metal markets, leading to improved investment decisions.

Subsequently, the study employs the MF-X-DMA for multifractal time series with significant coherence, confirming the presence of multifractal cross-correlation between gold and platinum at all scales. In spite of lower correlations, the two commodities still display long-term power-law cross-correlation, a finding of immense value for diversified investment portfolios.

The study finishes with a notable affirmation of the MF-X-DMA approach's superiority to the MF-DFA technique in reliably detecting long-term memory in co-movement time series. The combination of continuous wavelet transform (CWT) and MF-X-DMA methodologies provides new insights into the true dynamics of the gold and platinum markets, helping to shape future investment strategies and risk management procedures.

Key words: Gold; Platinum; Co-movement; Wavelet Coherency; MF-DFA; MF-X-DMA; DCCA; Multifractality; Vector FARIMA; VARIMA.

ÖZET

Bu tez, kıymetli metal fiyatlarını ve bunların dinamik ilişkilerini karakterize eden çoklu fraktal yapıyı kapsamlı bir şekilde araştırmaktadır. Vektörel Özbağlanımlı fraksiyonlu bütünleşmiş hareketli ortalama (V-FARIMA) modellemesi ve Çoklu fraktal Çapraz Korelasyon Trendsiz Hareketli Ortalama Analizi (MF-X-DMA) gibi gelişmiş teknikleri kullanan araştırma, emtia yatırımlarında tahmin doğruluğu ve risk-getiri değiş tokuşuna ilişkin kritik içgörüler sunuyor . Araştırmanın ilk kısmı, finansal istikrarsızlık dönemlerine özel bir vurgu yaparak, değerli metal fiyatlarının doğasında bulunan çoklu fraktal yapıya odaklanır. Bu aşamada toplanan içgörüler, emtia fiyat değişimleri için kesin tahminler oluşturmaya önemli ölçüde katkıda bulunur, yatırımcıları bilgili kararlar alma, riskleri etkin bir şekilde yönetme ve çalkantılı bir piyasada bile yatırımlarını koruma konusunda güçlendirir. Çalışma daha sonra altın ve platin getiri oranları arasındaki dinamik ilişkiyi araştırıyor ve değişen frekanslar ve zaman dilimleri arasında önemli bağlantılar keşfediyor. Bu bulgu, emtia piyasalarında birlikte hareket etme kavramını destekleyerek risk yönetimini, portföy çeşitlendirme tekniklerini ve etkili ticaret stratejilerinin oluşumunu daha da etkiler. Bu araştırmadaki dikkate değer bir keşif, daha düşük frekanslarda Hölder katsayısındaki sabitliğin gösterdiği gibi, uzun süreler boyunca tutarlı ortak harekettir. Bu sonuç, yalnızca önerilen tahmin yaklaşımını doğrulamakla kalmaz, aynı zamanda alanda gelecekteki araştırmalar için potansiyel yollar da açar. İlk bölüm, çoklu fraktal özelliği gösteren kıymetli metal zaman serilerinin Hölder katsayılarını tahmin etmedeki üstünlüğünü vurgulayarak V-FARIMA modelinin etkinliğini sunar. V-FARIMA modeli, verilerdeki altta yatan trendleri ve modelleri tespit etme konusunda umut vaat ediyor, kıymetli metal piyasalarındaki fiyat hareketlerini daha iyi anlamamızı sağlıyor ve daha iyi yatırım kararlarına yol açıyor. Ardından, çalışma, tüm ölçeklerde altın ve platin arasında çoklu fraktal çapraz korelasyonun varlığını doğrulayan, önemli tutarlılığa sahip çoklu fraktal zaman serileri için MF-X-DMA'yı kullanır. Daha düşük korelasyonlara rağmen, iki emtia hala uzun vadeli güç yasası çapraz korelasyonu sergiliyor, bu da çeşitlendirilmiş yatırım portföyleri için çok büyük bir değer bulgusu sağlamaktadır. Araştırma, MF-X-DMA'nın ortak hareket zaman serilerinde uzun süreli belleği doğru bir şekilde tespit etmede MF-DFA tekniği üzerindeki etkinliğini gösterir. Sürekli dalgacık dönüşümü (CWT) ve MF-X-DMA tekniklerinin entegrasyonu, gelecekteki yatırım stratejilerini ve risk yönetimi uygulamalarını şekillendirerek altın ve platin piyasalarının gerçek dinamiklerine ilişkin yeni bilgiler sunar.

Anahtar kelimeler: Altın; Platin; Eş hareketlilik; Dalgacık Uyumluluğu; MF-DFA; MF-X-DMA; DCCA; Çoklu Fraktallar; Vektör FARIMA; VARIMA.

To my precious Mother

ACKNOWLEDGMENTS

I would like to express my deepest appreciation to my late advisor, Professor Gazanfer Ünal. He was the torchbearer on this intellectual journey, guiding me with his illuminating insights and indomitable spirit. His profound understanding of how to integrate diverse disciplines has broadened my horizons and encouraged me to make my mark in the field of financial economics. His invaluable mentorship and unwavering support will forever be remembered.

I am tremendously grateful to my current advisor, Professor Erkut Akkartal, and co-advisor, Dr. Nida Türegün. Their continual support, meticulous feedback, and professional guidance have been of immense importance to the successful completion of this doctorate thesis. I would also like to extend my heartfelt thanks to all the committee members for their constructive critiques and encouragement throughout this process.

My sincere thanks go to my friends Tunç Oygur and Cengiz Karataş. Their friendship, support, and shared enthusiasm for knowledge and discovery have been a constant source of motivation throughout this journey. They have truly made this experience more rewarding and enjoyable.

Finally, I cannot overstate my gratitude to my family. Their endless support, patience, and understanding have been the foundation for this work. They have always believed in me, even during times when I found it hard to believe in myself. I dedicate this thesis to them, with all my love and respect.

In conclusion, this journey, while challenging, has been made brighter and more meaningful due to the collective effort and support of all those mentioned. My heartfelt gratitude to each one of them.

TABLE OF CONTENTS

LIST OF TABLES

LIST OF FIGURES

1. Multifractal Behavior in Precious Metals: Wavelet Coherency and Forecasting by VARIMA and V-FARIMA Models

Summary

This doctoral dissertation introduces a unique method to improve the precision of forecasting financial time series, especially in times of financial turbulence. The research underscores the potential opportunities in alternative investments that commodities, particularly precious metals, provide for financial experts. These resources are fundamental for portfolio diversification during regular financial crises characterized by intense volatility and contagion effects, often offering superior returns during bear markets for securities.

The primary focus of the study is a comprehensive examination of multifractal properties and the dynamic relationships of spot price returns on essential precious metals, primarily focusing on gold and platinum. A pioneering technique that incorporates the use of Hölder exponents in multifractal time series has been devised, allowing for a more accurate detection of vital swings during periods of financial distress. This groundbreaking methodology assists in capturing the multifractal behavior of financial markets, providing priceless insights into time-dependent market variances.

Additionally, this study surpasses conventional methods by scrutinizing the co-movement patterns in Hölder exponent time series, which exhibit unique multifractal patterns. The investigation substantiates the multifractal nature of the dataset and lays the groundwork for more precise projection of Hölder exponents in precious metal time series that shows multifractal features over consistent time spans.

This chapter's centerpiece is its cutting-edge strategy for forecasting prospective variations in commodity return rates, specifically during financial calamities. The outcomes emphasize the remarkable improvement in forecasting capability when adopting Vector Autoregressive Fractionally Integrated Moving Average (V-FARIMA) and Vector Autoregressive Integrated Moving Average (VARIMA) models for the multiple wavelet coherence of Hölder exponents within multifractal commodity time series. This discovery underscores the superiority of vector autoregressive models over univariate equivalents, culminating in a more comprehensive understanding of financial time series forecasting.

1.1 Introduction

Commodities offer a distinct avenue for investment to financial analysts, providing a buffer against the impacts of a financial crisis. Observations over the past two decades have revealed characteristics common to financial crises, such as significant volatility and the effect of contagion. These events, in turn, intensify the interconnectedness of worldwide equity markets (Sensoy, 2013). Concurrently, investors often favor these assets as a means of insulating their portfolios against the immediate fluctuations brought on by financial turmoil. Hence, the application of Hölder exponents in the analysis of multifractal time series of precious metals presents a chance for precise forecasting outcomes in vector fractional autoregressive models.

Investors often look for alternative investment opportunities during financial crises to avoid the high volatility and contagion effects that have become common features of these events in the past two decades. Precious metals are a popular choice for investors as they are considered a safe haven asset and can help preserve portfolios from instantaneous fluctuations caused by financial crises.

We discovered that employing Hölder exponents of multifractal precious metal time series can lead to accurate prediction outcomes in vector fractional autoregressive models. Hölder exponents are used to quantify the roughness or smoothness of a time series and have been demonstrated to be effective in predicting the volatility of precious metal prices. Researchers were able to increase the accuracy of their predictions for these commodities by including these exponents into autoregressive models.

The employment of vector fractional autoregressive models with Hölder exponents, in particular, has shown promise in predicting the volatility of precious metal prices. These models have been used to evaluate the behavior of precious metals such as gold and silver, with promising results in precisely forecasting price movements.

As a hedge against inflation and market volatility, commodities, especially precious metals, are a well-established strategy for investors. By incorporating the use of Hölder exponents and vector fractional autoregressive models, researchers have been able to improve the accuracy of their predictions for these commodities, providing investors with more reliable information to make informed decisions.

Therefore, primary commodities, namely gold, silver, and platinum, have emerged as suitable financial assets for diversification of investment portfolios (Sensoy, 2013). Echoing this, Chow and colleagues (Chow et al., 1999) proposed that commodities gain attractiveness under unfavorable financial conditions. Edwards & Caglayan, (2001) further validate this perspective by showcasing that commodity funds yield greater returns when equity performance is weak. Given these insights, this study has selected gold and platinum due to their reputation as reliable assets amid periods of financial instability. Moreover, the ability of precious metals to hedge due to their low connectivity with equity markets heightens their appeal (Hillier et al., 2006).

In recent years, financial crises have become more frequent and severe, causing high volatility and contagion effects in the equity markets. Thus, investors are increasingly seeking alternative investment opportunities that can protect them from the sudden fluctuations caused by these crises. Since precious metals, such as gold and platinum, do not correlate with equity markets, they have become popular among investors.

In this chapter, we demonstrated how using Hölder exponents of precious metal time series that shows multifractal features can lead to accurate prediction outcomes in vector fractional autoregressive models. Hölder exponents are a measure of a time series' roughness or smoothness and have been demonstrated to be effective in predicting the volatility of precious metal prices. We were able to increase the accuracy of these commodities' predictions by adding these exponents into autoregressive models.

In particular, the use of vector fractional autoregressive models that incorporate Hölder exponents has shown promise in predicting the volatility of precious metal prices. These models have been used to analyze the behavior of precious metals such as gold and silver and have shown promising results in accurately predicting price changes.

Additionally, commodities, especially precious metals, have been used as inflation hedges. Incorporating the use of Hölder exponents and vector fractional autoregressive models in the analysis of precious metals can provide investors with more reliable information to make informed decisions.

When the economy is in turmoil, it is usual to regard precious metals such as gold and platinum as safe haven assets. They are appealing to investors due to their minimal connection with equity markets. Furthermore, commodities, particularly precious metals, have been shown to be more appealing during bad economic times, offering larger returns when stocks perform poorly. Including commodities, particularly precious metals, in investing portfolios can therefore give diversification benefits as well as operate as a buffer against market volatility and inflation.

Overall, investors may find it beneficial to consider incorporating commodities, specifically precious metals, into their investment portfolios. The use of Hölder exponents and vector fractional autoregressive models can provide more accurate predictions for these commodities, enabling investors to make informed decisions.

The goal of this study is to look into the multifractal properties and dynamic connections in the return on spot prices of precious metals, notably gold and platinum. These metals are often viewed as safe investment assets, generating a lot of attention from investors. The Fourier transform is a prominent tool for studying these time series. Most financial time series analysis are performed in either the time or frequency domain. Traditional financial time series studies often focus on either time or frequency aspects, employing Fourier transform as a common technique for such data exploration. However, the Fourier transform lacks the ability to keep simultaneous time and frequency data, implying that a new method is required to examine non-stationary financial time series. The Fourier transform is not capable of maintaining both time and frequency information at the same time. As a result, the wavelet approach was developed to examine non-stationary financial time series (Burrus et al., 1998). To address this requirement, the wavelet method was developed, offering an advantageous mechanism to examine localized intermittent periodicities in the time-frequency realm, thus mitigating the shortcomings of the Fourier transform (Gülerce & Ünal, 2016). Wavelet transforms allow for the expansion of time series into time-frequency space, identifying localized intermittent periodicities and, as a result, overcoming the constraints of the Fourier transform. Wavelet coherence is used to find the co-movement zones of two-time series in the time-frequency domain, which proved to be a useful method for detecting precious metal correlations. The Hölder exponent quantifies the temporal fluctuations of financial instruments within the same market, and hence, is utilized to identify long-standing inaccuracies or distortions in the commodity market.

The primary goal of this research is to address longstanding inaccuracies or distortions in the commodity market using the Hölder exponent, a tool that quantifies temporal variations of financial instruments within the same sphere. The Hölder exponent's ability to discern the multifractal aspects of data and identify long-memory characteristics within it aids in accurately predicting significant shifts in financial time series. Moreover, the research highlights that vector autoregressive (VAR) models outperform univariate models, underlining their effectiveness in tracking the intricate dynamics of multifractal time series (Grech & Pamuła, 2008).

A distinctive aspect of this paper is its utilization of Hölder exponents to project future movements in commodity returns, especially during financial crises. Earlier studies focusing on the correlation of precious metal price time series (Oral & Unal, 2017a) primarily employed the vector autoregressive moving average (VARMA) models without accounting for their multifractality and long-memory attributes. Building on this groundwork, the current study advances this line of inquiry by investigating the correlation of Hölder exponent time series, which demonstrate unique patterns tied to multifractals. By proving the presence of multifractality in the data, the study sets the stage for its main investigation, which includes data multifractality, Hölder exponent time series, Hölder exponent correlation, and Hölder exponent prediction.

The following is how the paper is structured: Section 2 provides a thorough examination of the methods employed, specifically Multifractal Detrended Fluctuation Analysis (MFDFA), Wavelet Coherence, and V-FARIMA. Section 3 offers descriptive statistics for the time series, followed by an assessment of the MFDFA and Wavelet Coherence outcomes using Ihlen and Grinsted's respective toolboxes. Section 4 compares multivariate and univariate models, including the forecasting results derived from both model types.

Through this multifractal and co-movement investigation within the precious metals market, the research seeks to improve the forecasting accuracy of financial time series, particularly during discontinuous periods like financial crises. The application of Hölder exponents in forecasting forthcoming commodity returns introduces a pioneering approach, heightening prediction accuracy during financial instability.

Our fundamental aim is to enhance financial time series forecasting during discontinuity periods, namely, financial crises. Identifying the most accurate model to predict significant movements of the financial time series is crucial for investors seeking to make educated investment choices. This is particularly vital for time series possessing multifractal properties, implying data with long memory. Moreover, proving that vector autoregressive models yield more convincing results than univariate models is essential for the advancement of precise financial forecasting models.

Recognizing the relationships between gold and platinum can provide investors with insights into the movements of these two assets, leading to improved investment decisions. This chapter's findings can also aid policymakers responsible for commodity market regulation. By identifying inaccuracies or market distortions, they can implement suitable measures to stabilize the market and avert financial crises.

This study emphasizes the need of employing the wavelet technique to examine non-stationary financial time series and the Hölder exponent to quantify temporal fluctuations of instruments in the same market. The study's findings can guide investors towards making informed investment choices and aid policymakers in commodity market regulation. Future research can explore the multifractal features and dynamic correlations of other precious metals or assets and strive to create more accurate forecasting models for financial time series.

1.2 Methodology

1.2.1 Multifractal Detrended Fluctuation Analysis

The multifractal detrended fluctuation analysis (MF-DFA) is a valuable tool for estimating the Hölder exponents on the fluctuations of prices. These exponents can be used to calculate the singularity spectrum, which can then be used to calculate the multifractality of a financial time series. This is significant because understanding a time series' multifractal features might help us make better forecasts about future market behavior.

Kantelhardt et al., (2002) give a detailed process for doing MF-DFA, which comprises of five steps in their foundational publication. These steps are required to correctly evaluate a financial time series and produce useful results. However, it is worth noting that while MF-DFA is a powerful technique, it is not a panacea for all problems related to financial time series analysis. It is one of the tools that analysts can use to gain insights into market behavior and make informed trading decisions.

Moreover, it is important to recognize that financial markets are complex systems subject to various influences, including economic, political, and social factors.

Therefore, any financial time series analysis must consider these various influences and their potential impact on market behavior. MF-DFA, on the other hand, is a valuable tool that can offer analysts a greater understanding of the multifractal features of financial time series, allowing them to make more informed trading decisions. In these publications, the MF-DFA technique is broken down into five parts.

First, determine the integrated signal profile for a given time series

$$Y(i) = \sum_{K=1}^{i} \left| x_K - \langle x \rangle \right|, \quad i=1,...,N. \tag{1.1}$$

Subtraction of the mean $\langle x \rangle$ is optional. The integrated time series is then segmented into $N_s = int(\frac{N}{s})$ non-overlapping segments of equal length s in the following step. Because the length N of the series is frequently not a multiple of the time scale s evaluated, a short section near the end of the profile may remain. To avoid ignoring this section of the series, the identical approach is followed starting at the opposite end. As a result, $2N_s$ segments are obtained in total.

In the third phase, the least square fit of the series is used to calculate the local trend of each $2N_s$ segment. The variance for all segments is then calculated.

$$F^2(s,v) = \frac{1}{s}\sum_{i=1}^{s}\{Y[(v-1)s+i] - y_v(i)\}^2, \tag{1.2}$$

for each segment v, $v = 1, \ldots, N_s$ and

$$F^2(s,v) = \frac{1}{s}\sum_{i=1}^{s}\{Y[N-(v-N_s)s+i] - y_v(i)\}^2, \tag{1.3}$$

$v = N_s + 1, \ldots, 2N_s$ for each segment. In this case, the fitting polynomial in segment v is $y_v(i)$. The q-th order fluctuation function is then obtained by averaging all segments.

$$F_q(s) = \left\{\frac{1}{2N_s}\sum_{v=1}^{2N_s}\left[F^2(s,v)\right]^{\frac{q}{2}}\right\}^{\frac{1}{q}} \tag{1.4}$$

In general, the index variable q can be any real number other than zero. The power-law dependency of the q-th order moment of the fluctuation $F_q(s)$ in time series intervals s yields an estimate of the Hurst exponent $h(q)$, i.e.,

In general, the exponent h_q will be affected by q. h_2 is the well-defined Hurst exponent H for stationary series. As a result, we refer to h_q as the generalized Hurst exponent. The monofractal series is characterized by h_q being independent of q. Because of the uneven scaling of small and big fluctuations, h_q has a substantial dependence on q. For positive q, the segments v with the highest variance (i.e., the ones that deviate the most from the associated fit) will dominate the average $F_q(s)$. As a result, if q is positive, h_q represents the scaling behavior of segments with substantial fluctuations, and high fluctuations are often characterized by a smaller scaling exponent h_q for multifractal time series. When q is negative, the segments v with the lowest variance will dominate the average $F_q(s)$. As a result, for negative q values, the scaling exponent hq represents the scaling behavior of segments with small fluctuations, which are typically characterized by large scaling exponents (Ying et al., 2009).

Understanding how it scales time series is important for a variety of applications, including financial modeling, hydrology, and geophysics. Researchers have previously concentrated on monofractal time series, which a single scaling exponent may characterize. Much real-world time series, on the other hand, display multifractal behavior, indicating that the scaling exponent varies with the observation scale. As a result, having a generalized Hurst exponent that can capture the scaling pattern of multifractal time series is critical.

The dependence of h_q on q is a fundamental property of multifractal time series and can be used to characterize their scaling behavior. For positive q, the segments with substantial variations will dominate the average, and h_q will reflect their scaling behavior. For negative q values, the segments with small fluctuations will dominate the average, and h_q will represent their scaling behavior. The scaling exponent of segments with small fluctuations is frequently greater than the scaling exponent of segments with big fluctuations, resulting in a non-linear connection between h_q and q.

In summary, the generalized Hurst exponent h_q is an important tool for describing the scaling behavior of multifractal time series. Its reliance on q sheds light on the scaling patterns of segments with varying degrees of volatility. The study of multifractal time series is an important area of research, with applications ranging from physics to engineering to finance.

1.2.2 Wavelet Analysis

Wavelet transforms enable the localization of frequency decomposition and provide insights into frequency components. A wavelet is a function with the properties of integrable, has a zero mean, and exhibits frequency and time localisation. There are various wavelet families, each with its own set of qualities and characteristics. Daubechies, Coiflets, Symlets, and Haar are examples of common families. Each family has a variable amount of vanishing moments, which influences the wavelet's smoothness. The wavelet transform's accuracy is also affected by the number of vanishing moments.

Wavelet analysis is a strong method for evaluating non-stationary frequency data. It enables us to pinpoint frequency breakdown and generates frequency component information. Wavelets are a class of mathematical functions used to analyze signals and extract frequency content information. They are time and frequency localized, making them ideal for evaluating non-stationary signals such as speech, music, and biological signals.

There are several families of wavelets, each with a different set of properties and characteristics. Some common families include Daubechies, Coiflets, Symlets, and Haar. Each family has a variable amount of vanishing moments, which influences the wavelet's smoothness. The wavelet transform's accuracy is also affected by the number of vanishing moments.

Daubechies wavelets are orthogonal and have a compact support. They are commonly used in signal processing applications and have been shown to perform well in image compression. In her book "Ten Lectures on Wavelets," Ingrid Daubechies provides a detailed explanation of the Daubechies wavelets (Daubechies, 1992).

On the contrary, Coiflets are wavelets with a high degree of symmetry and a compact support. They are designed to be orthogonal and have been shown to perform well in image compression. Coifman and Wickerhauser, in their paper "Entropy-based algorithms for best basis selection," provide a detailed explanation of Coiflets (Daubechies, 1992).

Symlets are a family of orthogonal wavelets that are similar to Daubechies wavelets but have a higher degree of symmetry. They have been shown to perform well in image compression and other signal processing applications. Daubechies et al., in their paper

"An iterative thresholding algorithm for linear inverse problems with a sparsity constraint," provide a detailed explanation of Symlets (Daubechies, 2004).

The Haar wavelet is the simplest and most well-known wavelet. It is not orthogonal, but it has a simple structure and is easy to compute. It has been used in a variety of signal processing applications, including image compression. Mallat, in his book "A Wavelet Tour of Signal Processing," provides a detailed explanation of the Haar wavelet (Mallat, 2008).

The Morlet wavelet is a popular choice for wavelet analysis, especially for time-frequency analysis. It has a complex exponential function as its kernel, which makes it suitable for analyzing signals with oscillatory components. The parameter ω0 determines the central frequency of the wavelet and can be adjusted to match the frequency characteristics of the signal being analyzed (Grinsted et al., 2004).

Continuous wavelet transforms (CWT) are a technique for analyzing non-stationary frequency content in signals. In contrast to the discrete wavelet transform (DWT), which only offers information about specific frequency bands, the continuous wavelet transform (CWT) provides information about the frequency content of a signal at all points in time. This makes it ideal for assessing signals with variable frequency content over time, such as speech or music.

The CWT achieves this by breaking the signal down into wavelet components of varying sizes and locations. Each component is a wavelet function that has been scaled and shifted to cover a specific section of the time-frequency plane. A number of numerical approaches, including the Fast Wavelet Transform (FWT) and the Wavelet Packet Transform (WPT), can be used to compute the CWT.

One drawback of the CWT is that it can be computationally expensive, especially for long signals or high-resolution analyses. In addition, the interpretation of the CWT can be more complex than that of the DWT, since it involves examining the wavelet components at every point in time. However, for certain applications, such as speech or music analysis, the benefits of the CWT may outweigh its drawbacks.

In result, wavelet analysis is a diverse and powerful method for studying signals with non-stationary frequency content. Each wavelet family has its own set of qualities and characteristics, and the wavelet family chosen is determined by the application. The continuous wavelet transform is a sophisticated expansion of the discrete wavelet transform that offers information about a signal's frequency content at every point in time. It is, however, more computationally expensive and more difficult to interpret than the DWT.

The Morlet wavelet is a popular choice for wavelet analysis, especially for time-frequency analysis. It has a complex exponential function as its kernel, which makes it suitable for analyzing signals with oscillatory components. The parameter ω_0 specifies the wavelet's central frequency and can be changed to match the frequency characteristics of the signal under consideration.

Continuous wavelet transforms are a way to analyze signals with non-stationary frequency content. The CWT, as opposed to the DWT, offers information about the frequency content of a signal at every point in time. This makes it well-suited for analyzing signals with time-varying frequency content, such as speech or music.

One advantage of using the CWT over the DWT is that the CWT provides information about the frequency content of a signal at every point in time. This makes it well-suited for analyzing signals with time-varying frequency content, such as speech or music. In contrast, the DWT only provides information about specific frequency bands.

The CWT accomplishes this by decomposing the signal into wavelet components of various scales and positions. Each component corresponds to a wavelet function that is scaled and shifted to cover a particular portion of the time-frequency plane. A number of numerical approaches, including the Fast Wavelet Transform (FWT) and the Wavelet Packet Transform (WPT), can be used to compute the CWT.

One drawback of the CWT is that it can be computationally expensive, especially for long signals or high-resolution analyses. In addition, the interpretation of the CWT can be more complex than that of the DWT, since it involves examining the wavelet components at every point in time. However, for certain applications, such as speech or music analysis, the benefits of the CWT may outweigh its drawbacks.

The wavelet transforms allow to localize frequency decomposition and produces information about frequency components. A wavelet is an integrable function with a zero mean that is frequency and temporal localized. The Morlet wavelet (with ω0=6) is an effective choice for component extraction when utilizing wavelet analysis. It provides a good balance between temporal and frequency localisation (see Grinsted et al., (2004).

A wavelet function is defined as follows:

$$\psi_0(n) = \pi^{-1/4} e^{i\omega_0 n} e^{-1/2n^2}, \tag{1.5}$$

where ω_o is frequency and n is time.

The wavelet transformations function as band-pass filters, and the purpose for applying them to time series is that they can be deconstructed and then reassembled. The phase relation of a pair of time series with non-normal distributions is critiqued in this section.

The convolution defines CWT

$$W_x(\tau, s) = \frac{1}{\sqrt{s}} \sum_{t=1}^{N} x_t \psi^* \left(\frac{t-\tau}{s}\right), \tag{1.6}$$

where * denotes complex conjugate.

1.2.2.1 The Cross Wavelet Transform

The cross wavelet transform (XWT) of two time series x_n and y_n, is characterized as $W^{XY}(u,s)=W^X(u,s)W^{Y*}(u,s)$ (Torrence & Compo, 1998). The letter *u* represents a position index, and the letter *s* represents the scale. The cross wavelet power is defined as $|W_{xy}(u,s)|$ and represents the time series' local covariance at each scale.

The XWT is a powerful tool used to analyze two time series, *xn* and *yn*, and identify their common power and phase relationship. The XWT characterizes this relationship as $W^{XY}(u,s)=W^X(u,s)W^Y(u,s)^*$, where *u* is the position index and *s* is the scale. We can detect the local covariance of the time series at each scale by computing the cross wavelet power, $|W_{xy}(u,s)|$.

One of the benefits of using the XWT is that it allows us to further visualize the phase relationship between the two time series. This is achieved by calculating the phase difference between the time series, resulting in a phase-difference spectrum (PDS). The PDS provides valuable information about the relative phase relationship between the time series at different scales, which can help us better understand the underlying dynamics of the system being studied. (Torrence & Compo, 1998).

In short, the XWT is an effective technique for determining the common power and phase relationship between two time series. We can acquire insights into the underlying dynamics of the system being examined by visualizing the phase relationship using the PDS.

When using the XWT, keep in mind that it is a complicated instrument that necessitates a thorough understanding of wavelet analysis and time series analysis. Furthermore, the wavelet utilized in the analysis should be carefully considered, since this might have a considerable impact on the results obtained. The XWT, on the other hand, can be a valuable tool for getting insights into the link between two time series and the underlying dynamics of the system being examined when used correctly.

1.2.2.2 Wavelet Coherence

The wavelet coherence is a valuable tool for assessing the time-frequency relationship between two time series. It can find co-move areas in two time series using wavelet transform and cross-spectral analysis. The wavelet coherence computation generates a matrix that indicates the strength of the association between the two time series at each time and frequency point, providing a detailed perspective of the correlation structure.

Monte Carlo simulations were performed to generate confidence ranges in order to discover significant coherence. We may reject the null hypothesis that the two time series are uncorrelated by comparing the coherence value at each position in the matrix to the confidence interval. This method enables us to locate the co-move areas of the two time series by identifying sections of the matrix where the coherence is statistically significant.

In the time-frequency domain, wavelet coherence is used to detect co-move regions of two-time series. P.J. Webster, (1999) estimated the squared wavelet coherence coefficient as

$$R_S^2(u,s) = \frac{|S(s^{-1}W_{xy}(u,s)|^2}{S(s^{-1}|W_x(u,s)|^2)S(s^{-1}|W_y(u,s)|^2)}, \tag{1.7}$$

S is the smoothing operator. The coefficient values will be in the range of 0 and 1. If the value gets close to 1 (zero) it provides proof of strong (weak) correlation.

The coefficient values will be in the range of 0 to 1, with a value close to 1 indicating a high correlation and a value near to 0 indicating poor correlation. The smoothing operator is used to compute the squared wavelet coherence coefficient, which is a measure of coherence strength.

Overall, wavelet coherence analysis can help us comprehend the relationship between two time series and the co-move areas in the time-frequency domain. By recognizing considerable coherence, we can acquire insights into the correlation structure of the two time series and make better informed decisions.

1.2.2.3 Phase Angle

The discrepancies in wavelet coherence phase reflect details about the oscillation (cycles) delays between the two time series. The phase difference is calculated as

$$\psi_{xy}(\mathrm{u, s}) = tan^{-1}\left(\frac{I\{S((s^{-1}W_{xy}(u,s)))\}}{R\{S((s^{-1}W_{xy}(u,s)))\}}\right), \psi_{xy} \in [-\pi,\ \pi], \tag{1.8}$$

where I and R denote the imaginary and real sections of the power spectrum, respectively.

This formula compares two time series and determines the phase difference between them using wavelet coherence analysis. The phase difference demonstrates the timing and direction of the interaction between the two time series. The phase is graphically depicted by arrows on coherence plots, which can demonstrate the direction and intensity of the relationship between the time series.

Arrows on the coherence visualizations indicate phase. A zero phase difference suggests that the time series under consideration have co-movement. The arrows point to the right (left) if the time series have a positive (negative) correlation. Arrows pointing up indicate that the first time series is ahead of the second, while arrows pointing down indicate that the second time series is ahead of the first (Vacha and Barunik, 2013).

The wavelet coherence phase can be used to calculate the temporal lag between two time series. If the phase difference between the two time series is zero, they are regarded to be moving together. The first time series is ahead of the second if the phase difference is positive. If the phase difference is negative, it signifies that the second time series is ahead of the first. This knowledge can be used to make predictions about how the data will evolve in the future and to understand the link between two time series.

1.2.2.4 The Cone of Influence

The CWT in wavelet analysis can exhibit boundary artifacts due to the intrinsic poor localisation of wavelets in time. As a result of the discontinuity induced by the time series' finite duration, the wavelet power decreases considerably at the time series' edges, generally falling to e^{-2}. Because of this border effect, the wavelet analysis results may contain unexpected distortions.

One frequent technique is to pad the time series with enough zeroes before applying the wavelet transform. The boundary artifacts brought on by the discontinuity are reduced by zero-padding the time series, which improves the results of wavelet analysis.

Furthermore, researchers commonly employ a technique known as the Cone of Influence (COI) to more precisely define areas of valid investigation and interpretation. The areas of the time-frequency plane where the boundary effects from the CWT cannot be ignored are shown graphically in the COI. It serves to identify the regions where the results of the wavelet analysis can be less reliable because of the effect.

Researchers can visually identify the regions of the time-frequency plane where wavelet analysis should be interpreted with caution by adding the COI. This enables a more precise evaluation of the time series' localized characteristics and dynamics while taking into account any distortions that may be caused by its finite length and boundary effects. The concept of the COI offers a useful tool for carrying out reliable wavelet analysis and correctly interpreting the outcomes (Grinsted et al., 2004).

1.2.3 Vector FARIMA (V-FARIMA) Models

Vector Fractionally Integrated Autoregressive Moving Average models, often shortened to Vector FARIMA or V-ARFIMA, are an expansion of univariate FARIMA models into a multivariate context. These models find frequent application in areas such as econometrics and signal processing.

Univariate FARIMA models are distinguished for their capacity to represent time series with long memory, which means that correlations between observations decline at a rate slower than exponential decay. This characteristic of long memory is prevalent in many economic and financial time series, hence, making FARIMA models a fitting choice for these cases.

V-ARFIMA models represent a multivariate extension of this concept, enabling simultaneous modeling of multiple time series that are interrelated. In a V-ARFIMA model, each series is modeled as a function of its own historical values, the past values of other series in the model, and certain random error components. This property makes them particularly valuable in situations where the variables being studied exhibit intricate, interconnected relationships.

The estimation of V-ARFIMA models can be carried out using different methodologies, such as maximum likelihood estimation or the method of moments. These models are useful for prediction, simulation, and structural analysis of multivariate time series.

Despite their utility, V-ARFIMA models are comparatively more intricate and demand more computational resources than simpler models like ARIMA or VAR. Consequently, they're typically employed only when there's compelling theoretical or empirical evidence supporting their use.

It's vital to remember that statistical modeling is an intricate process that necessitates careful attention to the fundamental assumptions and characteristics of the data. Hence, it's always advised to seek the guidance of a statistician or data scientist when working with complex models like V-ARFIMA.

This study's main aim is to underline that V-FARIMA techniques lead to more solid estimations in fractal time series. In our thesis, we utilize the V-FARIMA Process as our prediction instrument to gather and implement the newfound knowledge, striving for highly precise results compared to existing algorithms focusing on interdependency of data series.

It's also easy to confirm that the use of wavelet transform contributes to better forecasting outcomes. This enhancement stems from the practice of data scraping at consistent frequencies, which in turn leads to time series with a higher degree of correlation.

The V-FARIMA approach conducts a careful examination of the data, basing its analysis on past values of linked variables. It predicts the future states of chosen interconnected time series variables all at once by formulating a vector, hence allowing for more accurate forecast outcomes.

The uniform frequency of data movement tends to decrease the values of deviation when integrating strongly correlated and multifractal data into a vector-based model.

The ARFIMA time series (p, d, q) process method, it can be expressed by ARFIMA (p, d, q), where *p* signifies the number of time delays of the autoregressive model, *d* represents the degree of differencing and '$d=H-\frac{1}{2}$', and *q* corresponds to the order of the moving-average model, it can be expressed in function terminology through a mean, μ, as follows:

$$\alpha (E) (1-E)^d (y_t-\mu) = \beta (E) \varepsilon_t, \varepsilon_t \sim \text{i.i.d.} (0, \sigma_\varepsilon^2) \tag{1.9}$$

E is backward shift operator,

$$\alpha (E) = 1- a_1E - \dots - a_pE^p \text{ and } \beta (E) = 1 + b_1E + \dots + b_qE^q , \tag{1.10}$$

$(1- E)^d$ is the fractional differentiation operator defined as,

$$(1-E) = \sum_{k=0}^{\infty} \binom{d}{k} (-E)^k = 1- dE + \frac{d(d-1)}{2!} E^2 - \dots \tag{1.11}$$

The V- FARIMA method of orders *p* and *q* is supported as a y_t, m dimensional time series' vector, in which $\alpha_0, \alpha_1, \alpha_2, ..., \alpha_p$ and $\beta_0, \beta_1, \beta_2, ..., \beta_q$ matrices of order m*m and ε_t constitute a vector of disturbance.

$\alpha(z) = 1- a_1z - \dots - a_pz^p$ and $\beta(z) = 1 + b_1z + \dots + b_qz^q$ are matrix valued polynomials.

The ARIMA model is created by arbitrarily limiting d to integer values. The ARFIMA process is said to have long memory, or long-range positive dependency, for $d \in (0,0.5)$.

1.3 Empirical Results

1.3.1 Data

The daily closing prices of spot gold (XAU) and spot platinum (XPT) are derived from Reuters and illustrated in Fig.1 from January 2000 to November 2017.

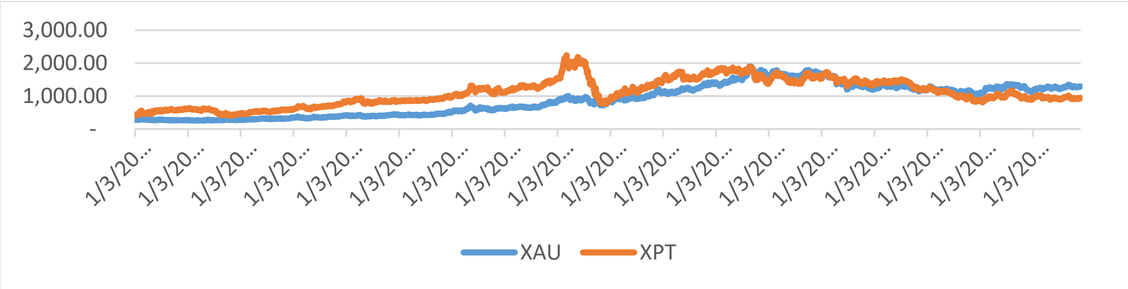

Figure 1. Spot gold price and spot platinum price

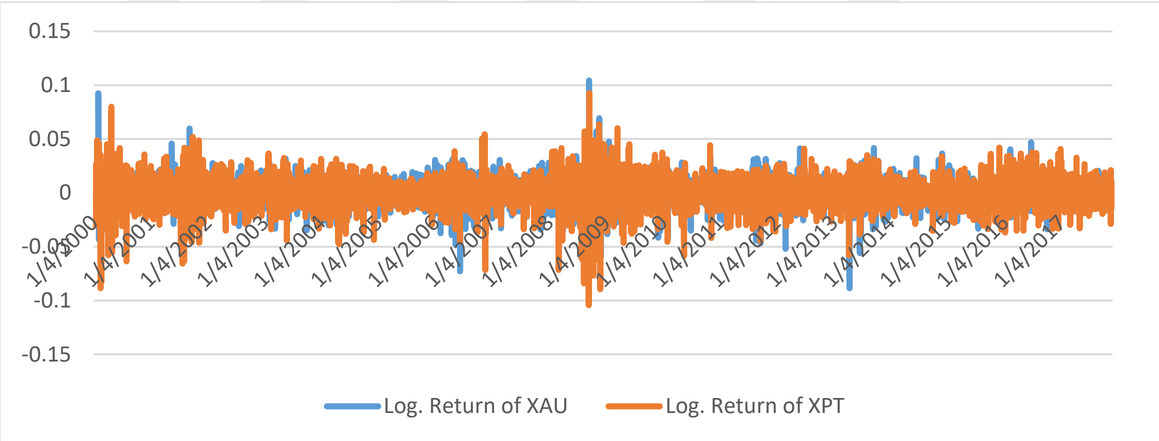

Figure 2. Logarithmic return of spot gold price and spot platinum price

Between 2000 and 2017, the spot prices of gold and platinum exhibited different patterns and trends. Spot prices refer to the current market prices at which these precious metals can be bought or sold for immediate delivery.

Gold, known for its status as a safe haven asset, experienced significant price movements during this time frame. In the early 2000s, gold prices were relatively subdued, ranging between $250 and $400 per ounce. However, as global economic uncertainties and geopolitical tensions increased, gold prices started a gradual upward trajectory. From around 2005 to 2011, gold experienced a remarkable bull run, with prices soaring to record highs. In 2011, gold reached its peak price of over $1,900 per ounce, driven by factors such as financial market turmoil, concerns over inflation, and monetary policy decisions. Following this peak, gold prices experienced a period of consolidation and correction, hovering around the $1,200 to $1,400 per ounce range until 2015. Toward the end of the period (2015-2017), gold prices became more volatile, impacted by variables such as the United States Federal Reserve's monetary policy decisions, geopolitical events, and global economic changes.

Platinum, another precious metal with various industrial applications, demonstrated a different price trajectory compared to gold during the same period. Platinum prices were generally higher than gold prices, reflecting its rarer and more specialized uses in industries such as automotive and jewelry manufacturing. In the early 2000s, platinum prices fluctuated between $500 and $1,000 per ounce. Similar to gold, platinum experienced a significant surge in prices from around 2005 to 2008, reaching a peak of over $2,200 per ounce. However, platinum prices faced a sharper decline than gold during the 2008 financial crisis, primarily due to its heavy reliance on industrial demand, particularly in the automotive sector. The prices of platinum remained relatively subdued in the subsequent years, fluctuating between $800 and $1,500 per ounce. Factors influencing platinum prices included changes in global automobile production, supply and demand dynamics, and economic conditions.

Economic indicators, geopolitical events, monetary policies, investor attitude, and market speculation can all have an impact on spot prices. Therefore, the fluctuations in spot gold and spot platinum prices between 2000 and 2017 were driven by a combination of global economic factors, market dynamics, and specific factors relevant to each metal.

The global financial crisis, which began in 2008 with the collapse of the subprime mortgage market in the United States, produced a huge structural breach in the worldwide financial landscape. This break impacted various markets, including the precious metals market.

In Figure 1, we can observe that spot gold and spot platinum prices showed structural break between 2008 and 2009. During this period, investors sought safe-haven assets to protect their portfolios from the financial turmoil and uncertainty. As a result, the structural break notably impacted spot gold and spot platinum prices.

The concept of structural breaks is crucial in time series analysis and econometrics. It aids in understanding anomalies in a series' continuity, which frequently manifest as abrupt and dramatic shifts that modify the series' fundamental characteristics. In the case of commodities such as gold and platinum, a structural break could indicate a significant change in market conditions that affects their pricing.

A structural break is a shift in a time series data set that results in a substantial change in the pattern of data. It's essentially a deviation from a long-term trend, often triggered by a significant event such as a policy change, technological innovation, or economic crisis. This shift has profound implications for data modeling, forecasting, and decision-making.

Regarding precious metals, structural breaks often reflect changes in the global economy and shifts in investor sentiment. For example, during periods of heightened economic uncertainty, the demand for gold, often considered a safe-haven asset, tends to increase, driving up its price.

Statistical techniques such as the Chow Test and the CUSUM (cumulative sum) test can be used to detect a structural break in gold and platinum prices. These tests are designed to detect rapid changes in the mean or variance of a time series.

Several instances of such breaks have occurred in the past. The breakdown of the Bretton Woods system, for example, in 1971 constituted a significant structural disruption for gold prices, as it removed the set $35 per ounce rate and allowed gold prices to fluctuate freely in international markets.

During times of crisis, gold, in particular, is frequently considered as a safe-haven asset, and its demand increases. This means that when other financial assets and markets are performing poorly, investors turn to gold as a way to safeguard their wealth. This increased demand leads to significant price appreciation, as investors view it as a reliable store of value amidst financial turbulence. The price of gold reached record highs during this period, surpassing the $1,000 per ounce mark and continuing its upward trajectory in subsequent years.

During the 2008 financial crisis, a huge structural breach occurred in the platinum market. The crisis led to a dramatic drop in automotive sales (as platinum is heavily used in the automotive industry for catalytic converters), resulting in a decrease in platinum demand and price.

Multiple factors can lead to a structural break in the prices of gold and platinum. These can include economic policies, financial crises, fluctuations in the dollar, shifts in industrial demands, geopolitical tensions, and changes in investment sentiment.

Monetary policies and inflation are key drivers that can lead to a structural break in gold prices. Because gold is generally regarded as a hedging tool against inflation, if central banks pursue expansionary monetary policies that result in increased inflation, demand for gold may rise, driving up its price.

For platinum, a structural break can occur due to shifts in industrial demand. As an industrial metal, the demand for platinum is strongly correlated with industrial and economic growth. Therefore, any significant changes in these areas, such as a recession or the emergence of new technologies that reduce its need, can cause a break in platinum prices.

The 2008-2009 structural break highlighted the divergent behavior between spot gold and spot platinum prices. While gold benefited from its safe-haven status and experienced a strong price rally, platinum faced headwinds due to its industrial reliance and the impact of the economic downturn on demand.

Structural breaks in the prices of gold and platinum have significant implications for investors, policymakers, and economists. For investors, these breaks can signal opportunities or threats, depending on their positions. For example, a rise in gold prices during a crisis can provide a profitable hedge for those holding gold. Conversely, a sudden drop in platinum prices might result in losses for those invested in platinum.

For policymakers and economists, understanding these breaks is crucial to decipher the underlying trends in the global economy. A surge in gold prices might indicate heightened economic uncertainty, while a drop in platinum prices could suggest a slowdown in industrial activity.

Structural breaks in the prices of gold and platinum provide valuable insights into the dynamics of the global economy and investor sentiment. Identifying these breaks and understanding their causes is crucial for informed investment decisions and effective economic policy-making. As the world economy continues to evolve, we can expect more structural breaks to occur, providing continuous learning opportunities for those keen on understanding the complex interplay between economics, finance, and commodities.

While the crisis had a significant impact on spot gold and spot platinum prices, the precise impact and timing of the structural breach can be impacted by a variety of factors. Market conditions, investor attitude, and the specific dynamics of the precious metals market, for example, are all elements that can influence the impact of a structural break on pricing.

Understanding the impact of a structural break on precious metals prices is crucial for investors, especially those seeking to invest in these metals, as a hedge against market volatility. By analyzing previous structural breaks and their impact on precious metals prices, investors can gain insights into potential market trends and make informed investment decisions

Table 1. *Descriptive Statistics of Log-Returns of Spot Prices*

	Mean	Median	Std.Dev.	Skewness	Kurtosis
XAU	0.0003	0.0004	0.0111	-0.1209	6.6008
XPT	0.0002	0.0007	0.0142	-0.4701	4.7950

According to a statistical examination of the data's logarithmic return, XPT returns are more volatile over this time period, as seen in Fig. 2 and Table 1. These differences could be driven by a variety of factors, including changes in XPT demand and supply, as well as market volatility. Despite these variations, both data sets show negative skewness, which means that the distribution of the data is skewed to the left.

When we analyze the correlation test findings for these two variables, we see that they have a correlation of 76 percent, which is quite high when considering the 17-year time period investigated. This suggests that there is strong correlation between the data, which could be the result of a number of causes, including those that are similar to both data sets.

We shall explore the connections between these data sets in more detail at the following sections. We will specifically look at the data's multifractal features and use wavelet coherence to identify the co-movement of those features. By doing so, we want to learn more about the underlying causes influencing the relationship between these data sets and find any potential patterns that could help guide future decisions.

1.3.2 MF-DFA Results

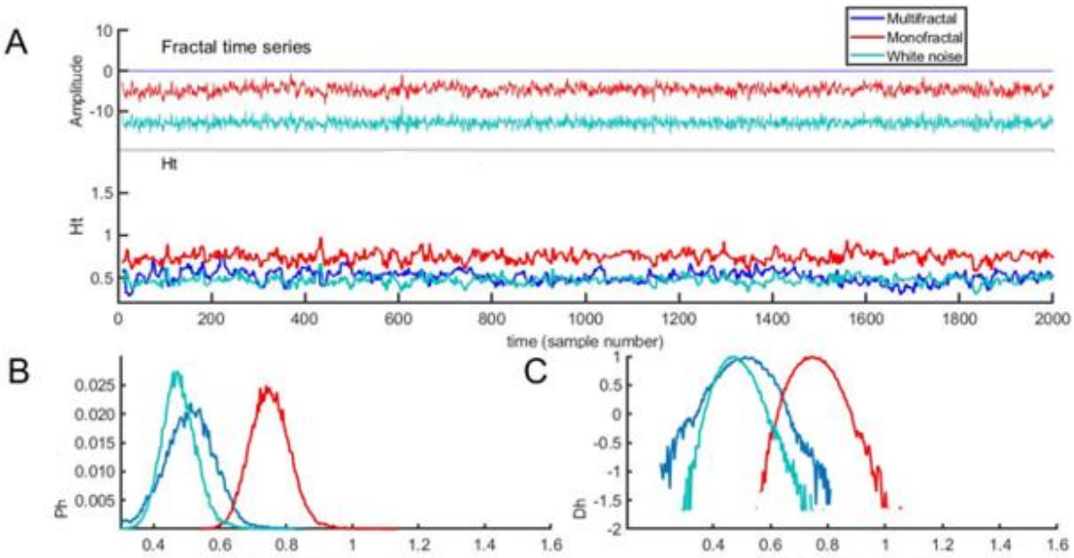

Figure 3. Hölder exponents of white noise, monofractal, and multifractal as log-return of gold spot price

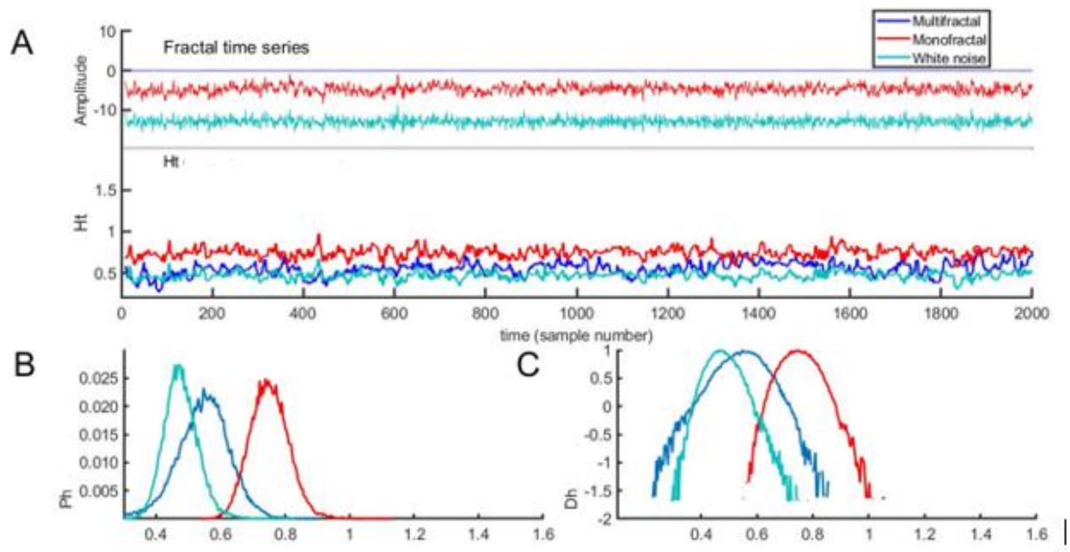

Figure 4. Hölder exponents of white noise, monofractal, and multifractal as log-return of gold spot price

In implementing MF-DFA, Ihlen's (2012) Matlab tools are used to indicate and interpret the results of precious metals return data. Fig.3 and Fig.4 show the multifractal, monofractal, and white noise time series (upper panel) and their Hölder exponents (lower panel).

The Hölder exponents for the monofractal time series are constant and equal to 1, while those for the white noise time series are random and have a mean of 0.5. The Hölder exponents for the multifractal time series vary over time and have a wider range of values compared to the monofractal and white noise time series.

At all scales, monofractal time series have a constant and fixed degree of self-similarity, which means they have similar patterns. On the other hand, white noise time series have no self-similarity, and their values are completely random, with no association between them. The Hölder exponent is a measure of a time series' degree of self-similarity, with a value of 1 indicating perfect self-similarity and a value of 0.5 suggesting no self-similarity. The Hölder exponent for a white noise time series is predicted to have a mean value of 0.5, indicating that the time series has no structure. These characteristics of monofractal and white noise time series are significant in understanding the attributes of precious metals return data examined with MF-DFA.

The logarithmic return of gold prices is represented as multifractal in Fig.3, while the logarithmic return of platinum prices is shown as multifractal in Fig.4. The Hölder exponents vary more in the multifractal time series than in the monofractal and white noise time series. The period with the smallest magnitude local fluctuation in a multifractal time series has the greatest Ht, while the period with the biggest magnitude local fluctuation has the smallest Ht. (B) Histograms are used to estimate the probability distribution Ph of the Hölder exponents Ht for multifractal, monofractal, and white noise time series. (C) The distribution of the Ph for the same time series is used to estimate the multifractal spectrum Dh. The multifractal time series has a wider distribution Ph and spectrum Dh than the monofractal and white noise time series (Ihlen, 2012).

These results suggest that the prices of gold and platinum have multifractal properties, indicating that they have a complex and dynamic structure. It appears that the patterns of price fluctuations for these precious metals are more heterogeneous than those for monofractals and white noise time series because the Hölder exponents vary more, and the Ph and Dh are distributed more widely. The results of this study have implications for precious metals risk management and portfolio diversification methods.

1.3.3 Wavelet Coherence Results

Wavelet coherence analysis seeks to understand and investigate how correlations, or the strength and direction of links between variables, vary over a range of frequency and time periods. This powerful technique allows us to observe and scrutinize changes and patterns that are not readily apparent in raw data, by providing a visual representation of how correlations evolve over time and at different frequencies.

In the wavelet plot, which is the graphical outcome of wavelet coherence analysis, the x-axis and y-axis are used to represent time and frequency, respectively. The time-frequency domains in which correlations are strongest or most notable can be quickly and easily shown with this implementation. Consequently, the plot offers a thorough and instructive snapshot of the interactions between the two variables or series being examined.

A color gradient from yellow to blue is used in the wavelet plot to graphically convey the significance level, which is a crucial indicator of the statistical robustness and dependability of observed correlations. Higher correlation between variables is shown by a deeper shade of yellow. Users can quickly detect and identify periods of high correlation using this color-coding technique, which may indicate intriguing or noteworthy patterns in the data.

The cone of effect, on the other hand, is represented by the faded region around the plot's edges. This region marks the area where edge effects may cause analysis to become distorted, lowering the validity of the wavelet power spectrum. Analysts can use this as a reference because it highlights the areas where results should be interpreted cautiously.

The black-lined areas show a 5% significance level against red noise (Oral & Unal, 2017a). In statistical testing, the 5% significance level is a commonly used cutoff that indicates that the observed correlation is highly unlikely to have happened by chance.

Thus, correlations in these black-contoured areas are therefore statistically significant and call for more investigation.

Arrows in the graphic indicate the directionality and synchronization of the two time series under analysis. A positive correlation is implied when arrows point to the right, but a negative correlation is implied when they point to the left. Additionally, the vertical placement of the arrows can show whether one series tends to lead or trail the other. Arrows pointing upwards specifically indicate that, in the examined time-frequency domain, the first one of the time series comes before the second series. On the other hand, if the arrows are heading downward, the second time series is likely to be ahead of the first.

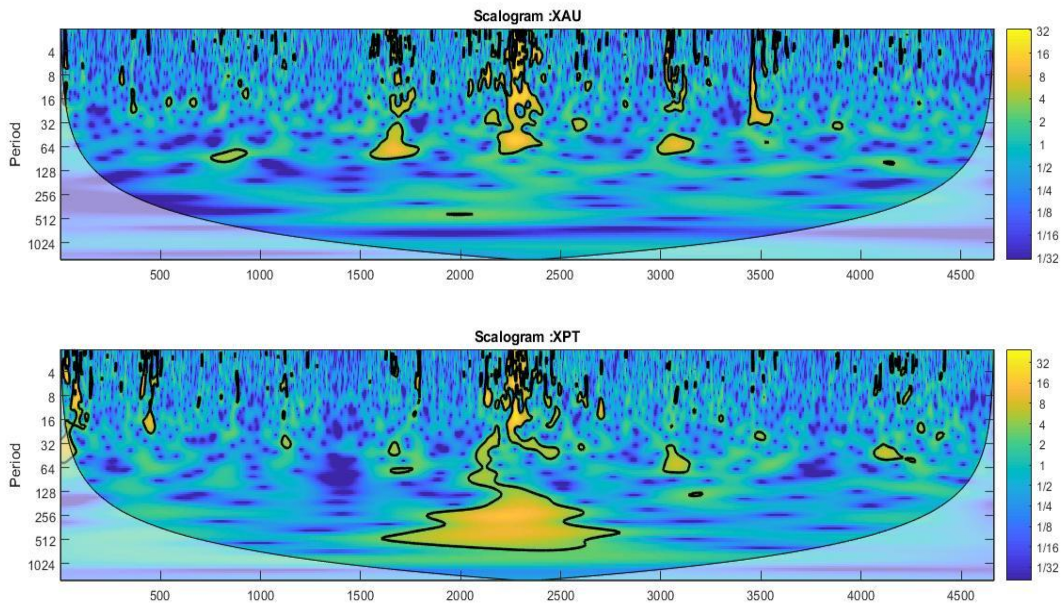

Figure 5. The wavelet power spectrum of XAU and XPT

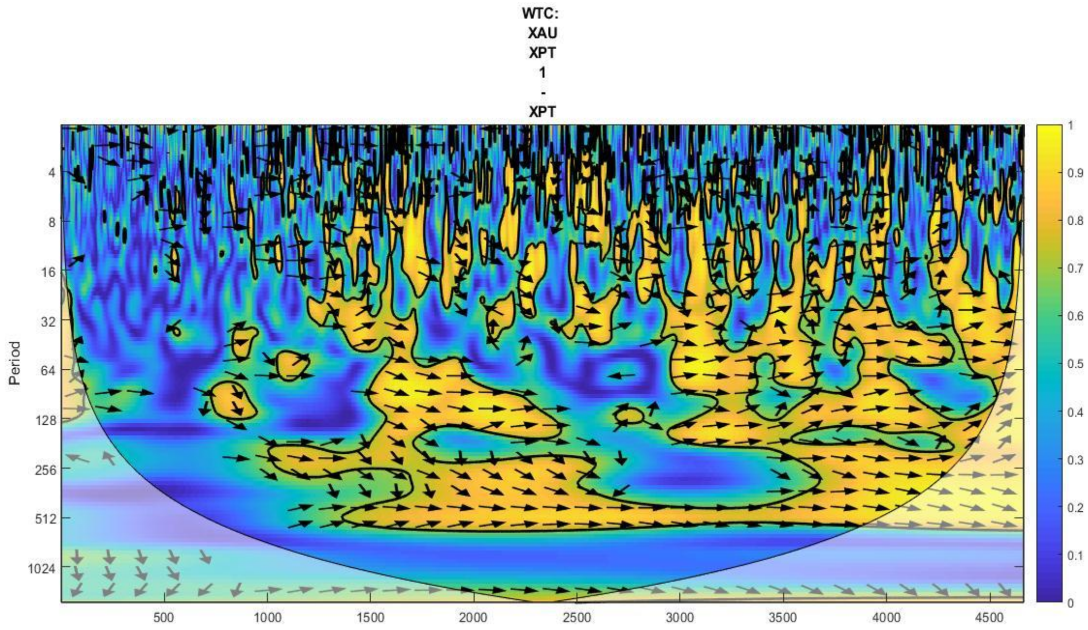

Figure 6. The WTC of XAU and XPT

The wavelet coherence analysis's outcomes for the spot gold and platinum price log returns are shown in Figure 6. In the figure, the black-lined yellow regions represent mostly significant coherent regions with glaringly high frequencies between 32 and 512.

According to the analysis, the most coherent time periods are from 06/10/2005 to 10/08/2009 and from 06/07/2011 to 07/04/2017. These results reveal that there was a strong correlation between the price changes of gold and platinum during these times, which may suggest that these two precious metals were subject to similar market forces.

The least coherent regions, on the other hand, are between 19/05/2000 and 10/09/2002, which are shown in blue at various frequencies. The price changes of gold and platinum were less connected during these times, indicating that the market forces affecting these two metals were not as coordinated.

When the phase relationship is considered, the wavelet coherence analysis reveals that almost all arrows point to the right, indicating that the two time series are in phase. This suggests that price changes in gold and platinum tend to occur at the same time. This strong correlation in price changes could be due to a number of factors, such as the use of both metals in jewelry or the economic forces that drive the demand for precious metals. It is also possible that this relationship is a result of the similar chemical properties of gold and platinum. Further research into the underlying causes of this correlation could help to shed light on the behavior of these two metals in the market and could be valuable for investors looking to diversify their portfolios.

For investors and traders who are interested in understanding more about the dynamics of the precious metals market, the wavelet coherence analysis offers useful insights on the relationship between the prices of gold and platinum.

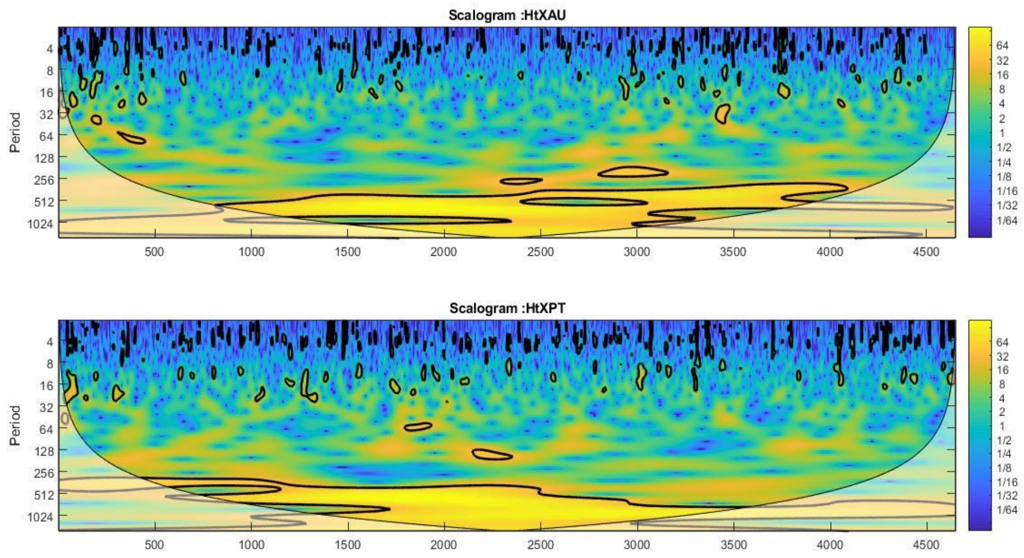

Figure 7. The wavelet power spectrum of local Hurst exponents of log-return spot price of both precious metal

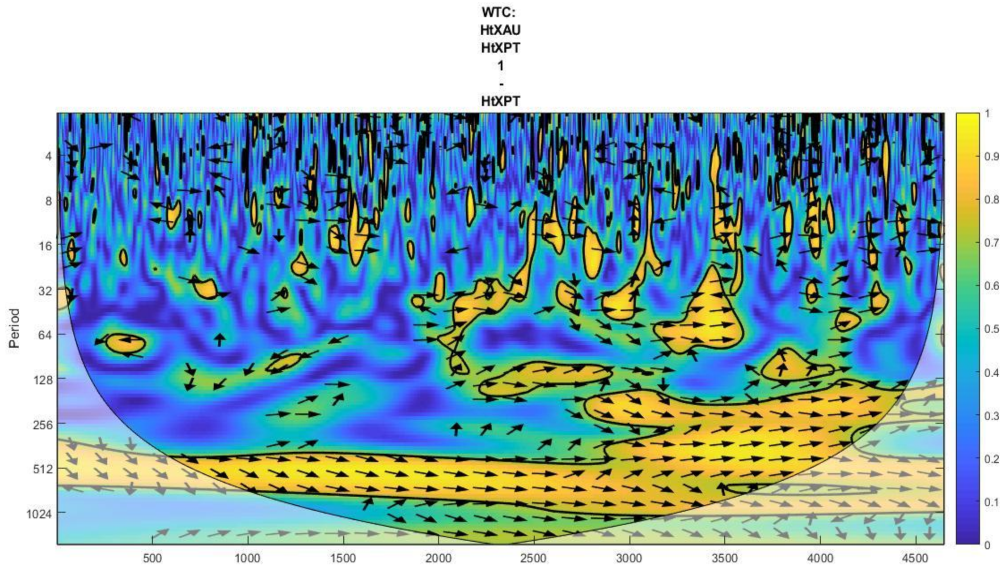

Figure 8. The WTC of local Hurst exponents of log-return spot price of both precious metal

Wavelet coherence results in Fig.8 indicate a highly significant association between the Local Hurst exponents of multifractal time series (logarithmic return of gold and platinum spot prices), particularly frequency around 512 across all time ranges. Furthermore, wavelet coherence shows that practically all arrows point to the right, implying that two time series are in phase. This means that the two series are moving together, and any changes in one series are reflected in the other series.

It is important to note that these findings provide insight into the behavior of the gold and platinum markets. According to the coherence between the two markets, changes in one market can have significant effects on the other. Understanding this relationship can help investors and analysts make more informed decisions when investing in these markets.

When two time series are not linear, wavelet coherence analysis can be a powerful tool for analyzing their relationship. This is because wavelet coherence can identify relationships that may not be apparent from traditional linear correlation analysis.

Gold and platinum market wavelet coherence analysis provide valuable information for investors and analysts. The findings show that two markets are intrinsically connected and that changes in one can have an impact on the other. Understanding this relationship allows investors to make more informed investment decisions, and analysts to better understand how these markets behave.

1.4 Multivariate ARIMA and Multivariate FARIMA Processes

In this study, multivariate autoregressive integrated moving average (ARIMA) and multivariate FARIMA processes are applied for the forecast, The goal is to deduce the discovered scene regarding interconnected relationships between time series in order to achieve high precision performance above previous methods. Multivariate processes are supposed to improve forecast accuracy by incorporating more interrelated variables (Granger, 1969). Multivariate models handle information in the past values of interconnected variables simultaneously in the forecasting of studied variables by creating a vector. As a result, more exact forecast performance is enabled.

By incorporating interrelated variables in the forecasting process, decision-makers can make more accurate predictions of future trends and patterns, resulting in better strategic decisions. When dealing with complex systems that are influenced by multiple variables, a more comprehensive understanding of their relationships can lead to better predictions. Therefore, by considering the relationships between time series, we can significantly improve the forecasting performance of multivariate models, as the results of this study have shown.

Moreover, the use of multivariate FARIMA models in this study has proven to be more effective regarding forecast accuracy than multivariate ARIMA models. The incorporation of interrelated variables in the forecasting process has led to a more precise prediction of the studied variables, which suggests that the use of multivariate models that consider the relationships between time series can significantly improve the accuracy of forecasts. This finding highlights the importance of incorporating interrelated variables in forecasting models, as it can lead to better predictions and, ultimately better decision-making.

Vector models have historically proven to be more difficult to implement. Vector models, on the other hand, offer clearer results in scenarios with two or more variables (Lütkepohl, 2004).

The Multivariate ARMA process is represented as follows:

$$A_0 y_t = A_1 y_{t-1} + A_2 y_{t-2} + \ldots + A_p y_{t-p} + M_0 \varepsilon_t + M_1 \varepsilon_{t-1} + M_2 \varepsilon_{t-2} + \cdots + M_q \varepsilon_{t-q} \qquad (1.9)$$

As a vector of y_t of m dimensional time series, the equation satisfies the multivariate ARMA process of orders p and q, in which $A_0, A_1, A_2, \ldots, A_p$ and $M_0, M_1, M_2, \ldots, M_q$ matrices of order m*m and ε_t is a disturbance vector.

If written in summary notation using lag operators,

$$\text{A(L)}y_t = \text{M(L)}\ \varepsilon_t, \text{ wherein,} \qquad (1.10)$$

A(z)= A_0-A_1z-…-A_pz^p and M(z)= M_0+M_1z+…+M_qz^q are matrix valued polynomials.

The zero-order matrices are often identical and they will be equal to the identity matrix,

$$A_0=M_0 = I_m \text{ (Lütkepohl, 2004).} \quad (1.11)$$

1.4.1 Forecast Results

As it is previously pointed out, the primary goal of this study is to demonstrate the improved forecasting techniques of multivariate ARIMA models over their univariate counterparts. The ability of multivariate time series models to effectively establish and numerically represent the high correlation between variables using wavelet analysis techniques is an essential quality (Oygur & Unal, 2017). Vector Autoregressive Integrated Moving Average (VARIMA) models are highly relevant in this situation. They provide a convenient framework for discerning the dynamic interrelationships between the variables in question (S.Tsay, 2013).

In this section, we will look in depth at the modeling and forecasting of gold and platinum prices. The models were fitted to the data and projected using both ARIMA and VARIMA methodologies. The best model was then chosen after a thorough evaluation of the confidence bands associated with each model's forecast results.

Examining the Wavelet Transform Coherence (WTC) plot reveals that the period with the highest correlation ranges from July 2011 to March 2015, in the 256-512 day range. This corresponds to an octave value of nine on the scalogram. Following the identification of the coherence time interim, the data was processed using a Continuous Wavelet Transform (CWT). This phase allows the data to be transformed into both time and frequency domains. An inverse CWT was used to isolate the relevant frequency following this transformation.

Following that, the inversed data relating to gold and platinum prices were integrated into a number of models, including ARIMA[1,1,1] and VARIMA[1,1,1], as well as FARIMA[3,0.2,1] and V-FARIMA[3,0.2,1]. The entire research was based on 950 data points, with forecasts for 70 of them given by each model. The subsequent results, depicted in Figures 9–12, show that the projections for both data sets exhibit outstanding consistency with the extracted return data. This can be attributed to the inherent characteristics of the extracted data coupled with the strong correlation between each vector of the time series (Oral & Unal, 2017a).

The crucial point of this research is that the multivariate models, specifically VARIMA and V-FARIMA, have significantly narrower confidence intervals in their forecasting data. This is due to the low covariance relationship of the matrices involved, which eventually improves the precision of the anticipated data and provides significant proof for the utility of multivariate models in forecasting these complex financial instruments.

The findings of the study have significant significance for financial analysts and investors wanting to make informed decisions about precious metals investments. Analysts can develop more accurate forecasts of gold and platinum prices by utilizing multivariate models such as VARIMA and V-FARIMA, which take advantage of the high correlation between variables and the dynamic interrelationships between them. These models can also provide a more comprehensive understanding of the complex nature of financial assets such as precious metals, which can be extremely volatile and susceptible to a wide range of external parameters.

One of multivariate models' primary characteristics is their capacity to uncover and represent complicated interactions between several variables, which can be difficult to express using univariate models. The study discovered, for example, that the V-FARIMA model was particularly good at capturing the significant correlation between gold and platinum prices from July 2011 to March 2015. Analysts were able to provide more accurate and precise projections of future pricing for both metals by including this information into the model.

Another significant finding of the study was the significant difference in confidence bands associated with multivariate models versus univariate models. The multivariate models' narrower confidence bands reflect higher precision in the anticipated data, which can be a useful tool for investors looking to make informed decisions about buying or selling precious metals. The study's findings imply that multivariate models like VARIMA and V-FARIMA can provide a more comprehensive and accurate understanding of the complex dynamics of financial assets like gold and platinum prices, making them a valuable tool for investors looking to maximize their returns.

Overall, our findings emphasize the need to employ advanced modeling techniques such as wavelet analysis and multivariate models in order to provide more accurate and exact forecasts of financial instruments like as precious metals. Analysts and investors can use these tools to better grasp the complex relationships between variables and make more informed investment decisions. The study's findings make a solid case for using multivariate models to forecast complex financial instruments, implying that additional research in this field could offer even more significant insights for investors and analysts alike.

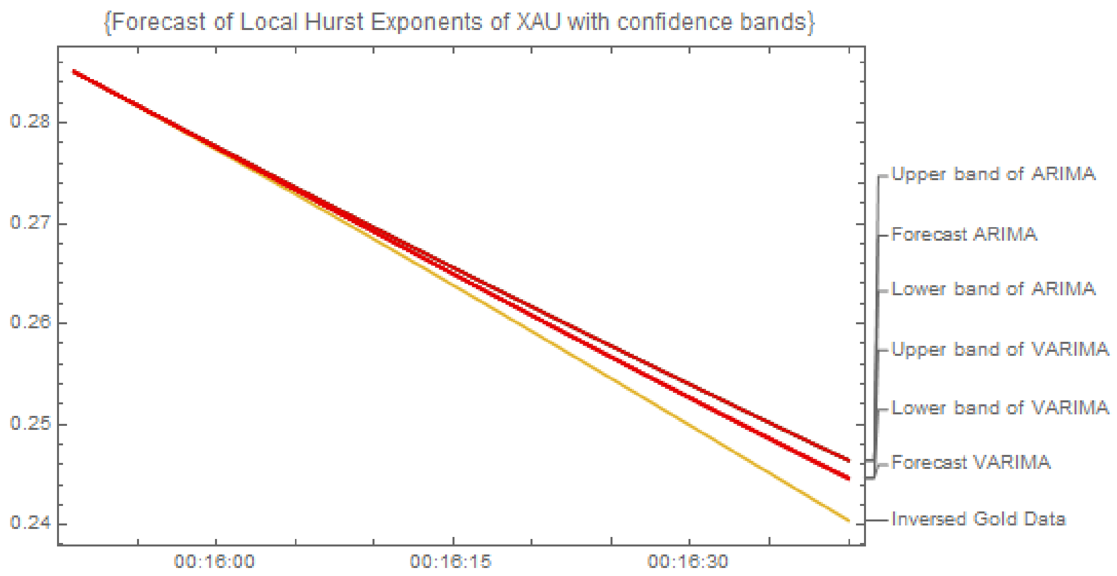

Figure 9. VARIMA [1,1,1] and ARIMA [1,1,1] comparison for Local Hurst Exponents of XAU

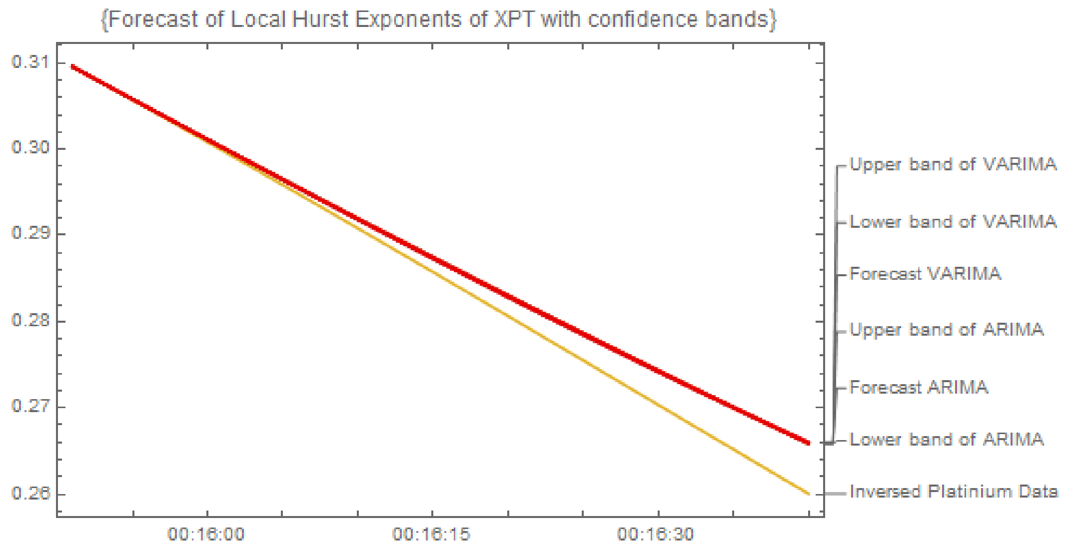

Figure 10. VARIMA [1,1,1] and ARIMA [1,1,1] comparison for Local Hurst Exponents of XPT

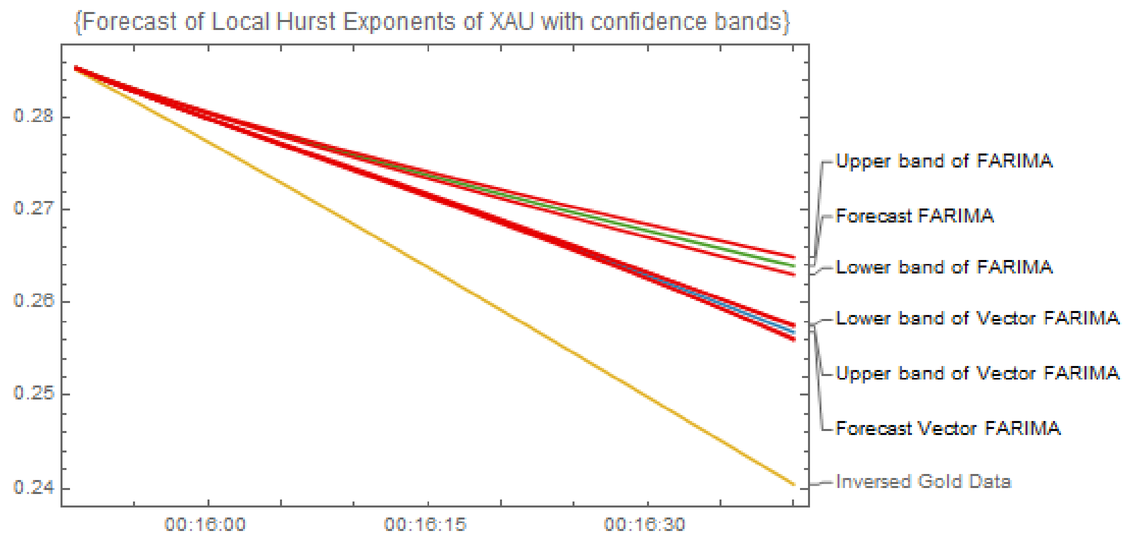

Figure 11. Vector FARIMA [3,0.2,1] and FARIMA [3,0.2,1] comparison for Local Hurst Exponents of XAU

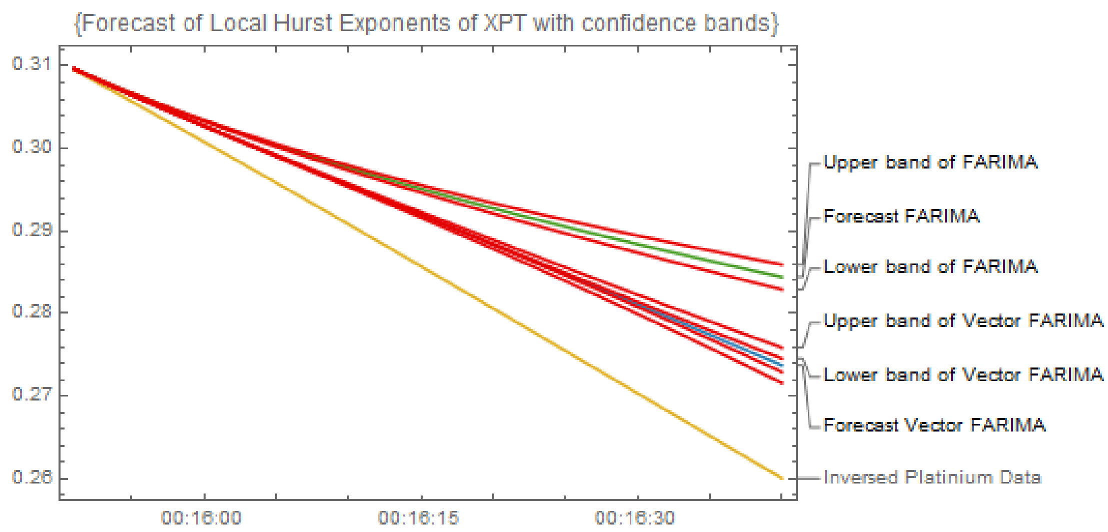

Figure 12. Vector FARIMA [3,0.2,1] and FARIMA [3,0.2,1] comparison for Local Hurst Exponents of XPT

1.5 Results

In this research, it is suggested that improving Vector Fractionally Integrated Autoregressive Moving Average (V-FARIMA) modeling and forecasting requires the utilization of multiple wavelet coherence of Hölder exponents for precious metal time series which are show multifractal features. Additionally, it clarifies three core issues, each of which contributes to improve the forecasting accuracy of Hölder exponents of precious metal time series, which are show multifractal features, when computed at correlated time scales, measured by the Wavelet Transform Coherence (WTC) method.

The initial focal point of this study is the exploration of the multifractal structure that characterizes precious metal prices data. Particularly during times of financial instability, this particular attribute is a crucial component in the construction of exact predictions for commodity price variations that could have a significant impact. Investors can develop more complex understandings of the risk-return tradeoff in commodities investments and develop more thorough financial crisis prediction models by understanding the dynamics of these price variations.

The importance of this asset resides in the fact that it provides a foundation for making precise projections and spotting market patterns that can be advantageous or harmful to investors. Making wise selections in a turbulent market like the commodities sector might be facilitated by this knowledge.

In a broader sense, this asset is essential in assisting investors in navigating the complex world of commodities investments by giving them the skills they need to make knowledgeable decisions, effectively manage their risks, and ultimately protect their investments.

The dynamic relationship between the return rates of gold and platinum is investigated in the next step. We identify coherent temporal intervals with Morlet Wavelet analysis and carefully evaluate these connections with the WTC approach. According to our research, there are substantial connections between the prices of platinum and gold across a range of frequencies and time frames.

These findings support the notion of co-movement behavior in commodities markets by illuminating the independent properties of each precious metal and their linked influences on one another. As a result, risk management and portfolio diversification techniques may benefit from our research. Investors who want to gain from co-movement behavior can think about having both gold and platinum in their portfolios. Trading decisions and effective strategies can also be developed using the observed correlations.

After carefully evaluating the WTC results of the original dataset, we decided to further investigate the WTC results of the Hölder exponents, which we had discussed in detail in the preceding sections of this paper. The Hölder exponents had significant constancy at lower frequencies, as we discovered after careful inspection. This was a noteworthy finding since it suggested that there was continuous comovement over long periods of time. This consistency not only supported our early observations of long-memory features, but it also increased the validity of our suggested forecasting approach. Furthermore, we think that these findings may have significant ramifications for present and future studies in this area. It could be interesting to investigate the source of this coherence in the Hölder exponents and see if similar results can be obtained in other datasets. We may also look into how this methodology might be used in other fields of study or even different industries.

The culmination of our findings is presented in the last section of Chapter 1. Our research shows that, when computed at coherent time intervals, the V-FARIMA model considerably increases the forecasting accuracy of the Hölder exponents of precious metal time series which are show multifractal features. In contrast, when using the ARIMA and VARIMA models to examine the Hölder exponent series during comovement, rather poor results were obtained. To further elaborate on this, it is worth noting that the V-FARIMA model incorporates both long-memory and short-memory components, which are critical in accurately modeling the complex dynamics of the multifractal time series.

The V-FARIMA model also makes it possible to spot underlying trends and patterns in the data that could be difficult to see with other models. Overall, the V-FARIMA model shows tremendous promise in successfully forecasting multifractal time series, which is an important point made by our study.

These results lead us to the conclusion that datasets with a long memory, like the Hölder exponent time series, are better suited to the V-FARIMA modeling and forecasting approach. By using this complicated yet precise strategy, we can increase the precision of future forecasts and our comprehension of price movements in the precious metal markets, which will ultimately lead to better investing decisions in these areas.

After analyzing the results, we can confidently say that datasets with a long memory, like the Hölder exponent time series, are better suited to the V-FARIMA modeling and forecasting approach. This complex yet precise strategy helps to increase the precision of future forecasts and our comprehension of price movements in the precious metal markets. We can make better-informed investing decisions in these areas by implementing this approach.

It is crucial to emphasize that, while this strategy has a lot of potential, it requires a lot of processing power and skill. However, it has the potential to be a game changer for financial institutions and other entities looking to improve their forecasting capabilities in the precious metal markets.

In conclusion, the V-FARIMA modeling and forecasting strategy has proven to be a reliable and successful way for anticipating precious metal market behavior. However, before using this strategy, fully understanding the principles and complications involved is critical. It is worth exploring if you have the appropriate experience and computational capability.

2. Exploring The Multifractality in the Precious Metal Market

Summary

Chapter two introduces a fresh method for exploring the multifractal features of time series via the multifractal cross-correlation detrended moving average analysis (MF-X-DMA). This research delineates the distinct reactions of MF-X-DMA during coherent and incoherent temporal stages. The absence of a process to detect the dynamic cross-correlation in time series creates a hurdle for analysis when dealing with time series that exhibit multifractal structures. However, the research reveals that the wavelet coherence technique, once implemented on time series, can effectively spot concurrent movements in certain temporal segments, thus providing a streamlined means to identify applicable intervals for MF-X-DMA. The wavelet coherence approach is applied to daily spot gold and platinum prices beginning in January 1987. The results reveal its prowess in isolating specific time series in particular frequency and temporal periods, thus obviating the necessity for windowing or shuffling approaches. Furthermore, utilizing detrended cross-correlation analysis coefficients of inverted series for both low and high-correlation series, the study records a long-term power law cross-correlation. Lastly, the research shows that, especially with highly correlated data, MF-X-DMA performs better than the MF-DFA.

2.1 Introduction

Forecasting financial crises and spotting market anomalies have grown significantly in recent years in the study of economics. For economists and policymakers, analysis of multifractal behavior has become an effective tool for identifying long-term memory and critical fluctuations. This analysis method has been used to examine the spot prices of platinum and gold, indicating their coherency and multifractal nature. These findings have significant implications for investors since they may be used to create better hedging and risk management plans, spot investment opportunities, and make smarter portfolio allocation strategies. Also, identifying these features of spot prices might help understand economic progress more precisely and effectively. Overall, examining the multifractality and coherency of spot prices has become increasingly essential to comprehend how financial markets behave and how they affect the broader economy.

Examining the multifractal nature of financial markets has garnered considerable attention from scholars. The interconnectedness among financial entities has been a focal point of many past investigations employing different approaches. Jiang et al., (2019) offered an extensive review of financial market multifractal analyses, spotlighting the broad array of methods and tactics used. Studies like the one conducted by Lin et al., (2018), which delved into the effects and links among global gold markets, have also delved into the cross-correlations in financial markets. Wang, (2017) and his colleagues' research is another excellent example, demonstrating the application of multiscale methodologies to scrutinize the fallout of the global financial crisis on stock market contagion. Furthermore, Xie et al., (2015) developed a joint multifractal analysis based on wavelet leaders to examine the interrelationships between various financial assets. Wang & Xie, (2013) investigated the relationship between China's CSI 300 index's spot and futures markets. Collectively, these studies offer invaluable insights into the multifractal aspects of financial markets and the assortment of analysis techniques available.

The technique of multifractal detrended analysis offers significant benefits in gauging the multifractality of time series. Meneveau and colleagues introduced the multifractal cross-correlation analysis (MF-X-PF), Jiang et al., (2017) as a method in 1990 to investigate the relationships between the dissipation rates of kinetic energy and passive scalar oscillations in fully mature turbulence (Meneveau et al., 1990). Dealing with the combined partition function of two multifractal measures was part of the approach. In a separate study, Wang and his colleagues investigated a related method known as the multifractal statistical moment cross-correlation analysis (MFSMXA) (J. Wang et al., 2012), which is a subset of the MF-X-PF. The multifractal formula for binomial measurements was developed and validated by Xie and colleagues. Kristoufek proposed the structure function-based multifractal height cross-correlation analysis (MF-HXA) (Kristoufek, 2011). Zhou transformed the detrended fluctuation analysis into the multifractal detrended cross-correlation analysis (MF-X-DFA) (Zhou, 2008), which is a multifractal adaption of the detrended cross-correlation analysis (DCCA) (Podobnik & Stanley, 2008). Jiang and Zhou combined multifractal detrending moving-average analysis (MF-DMA) with detrending moving-average analysis (DMA) to create the MF-X-DMA cross multifractal formulation. MFCCA and MFDPXA (such as MF-PX-DFA, MF-PX-DMA, and so on) are two other multifractal cross-correlation analysis methodologies. These methods have been useful in identifying long-term cross correlations between pairs of series from various financial markets (Jiang, Yang, et al., 2017).

It has been demonstrated that the MF-X-DMA can efficiently forecast the cross-correlation between two time series that show multifractal features. Numerous studies have charted the evolution of fluctuation analysis over the years. Peng and his colleagues (Peng, C.-K., Buldyrev, S. V., Goldberger, A. L., Havlin, S., Sciortino, F., Simons, M., & Stanley, 1992) pioneered the use of fluctuation analysis (FA) to detect abnormal oscillations in time series with minimal data sets. However, because most time series are non-stationary, they can only be used immediately after the trend has been neutralized. To solve this, detrended fluctuation analysis (DFA) for analyzing the autocorrelation of a non-stationary time series has been proposed (Peng, C.-K., Buldyrev, S. V., Havlin, S., Simons, M., Stanley, H. E., & Goldberger, 1994). DFA is classified into two categories. Kantelhardt et al. (Kantelhardt et al., 2002) introduced a variation, the multifractal DFA (MF-DFA), for studying multifractality in non-stationary time series. The detrended cross-correlation analysis (DCCA), proposed by Podobnik and Stanley (Podobnik & Stanley, 2008), investigates the power-law cross-correlation between two time series. Later, Zhou developed MF-DCCA to assess the higher-dimensional multifractal behavior of two time series (Zhou, 2008). DCCA has been widely used in a variety of disciplines, including financial markets (Cao et al., 2014), (G. J. Wang et al., 2014), highway traffic series (Dai et al., 2016), weather forecasts (Govindan et al., 2001), and coding and non-coding DNA sequences (Pal et al., 2015).

Gu & Zhou, (2006) adapted DFA and MF-DFA into higher-dimensional analogues. Drawing on DFA, Podobnik and Stanley developed a detrended cross-correlation study to investigate power-law cross-correlations between several simultaneously recorded time series using a non-stationarity detrending approach (Podobnik, Horvatic, et al., 2009)(Podobnik, Grosse, et al., 2009).

DFA and MF-DFA use polynomial fitting to remove existing trends in time series (Y. Wang et al., 2011). Gu and Zhou presented a novel set of MF-DMA in 2010 to widen the DMA approach by removing local trends by subtracting the local means (Gu & Zhou, 2010).

The utilization of wavelet transformation for exploring fractals and multifractals is a recognized technique (Holschneider, 1988), (Grasseau, 1988). A common strategy to deal with the finite size effect in multifractal analysis involves shuffling the time series or employing phase randomization algorithms, which successively eliminate linear and nonlinear correlations or the original time series distributions'. Nonetheless, these methods have their constraints as they may alter the fundamental traits of the signal (Gao et al., 2022). As a substitute, the continuous wavelet transform (CWT) can alleviate the finite size effect. The CWT is a scale-dependent method that surpasses the restrictions of a fixed window size by studying a signal across various scales. By applying CWT, more intricate details concerning a signal's multifractal behavior can be garnered by analyzing the signal's local properties at different scales.

In our paper, we suggest a novel method for examining the multifractality of time series by initially carrying out a wavelet analysis on our data. Compared to Fourier analysis, wavelet analysis computes the spectral attributes of a time series as a time-dependent function, facilitating a more intuitive local data analysis. Moreover, the Fourier transform tends to forfeit crucial time information, complicating the identification of temporary relationships or structural shifts. These restrictions render Fourier methods applicable only to stationary time series with constant statistical characteristics (Aguiar-Conraria & Soares, 2011).

We focus on daily spot prices of gold and platinum beginning in January 1987 to examine the performance of the MF-X-DMA during coherent and non-coherent time frames. To convert the data into frequencies, we use a scale-by-scale continuous wavelet transform. Following that, both MF-X-DMA and MF-DFA are used to investigate coherent and non-coherent time periods. Specifically, we assess the efficacy of using MF-X-DMA during coherence time periods by applying the wavelet coherence method. We also compare the outcomes of MF-DFA and MF-X-DMA for uncorrelated and correlated time periods at different sizes. Our research proves that the time series extracted using MF-X-DMA provides superior results for both time intervals.

The second chapter is formatted as follows. The data and methodology are presented in section 2. The next section contains descriptions and empirical results of the analysis, including the empirical results of the wavelet coherence, MF-X-DMA, DCCA, and Reyni exponents of the data. The fourth section compares the correlated and uncorrelated time periods. The final section, section 5, offers concluding remarks and discussions.

2.2 Data & Methodology

2.2.1 Data

Our research utilizes the spot prices of gold (XAU) and platinum (XPT) as precious metals. More precisely, XAU denotes the spot price of gold in US dollars, as determined by the trading activities in the worldwide over-the-counter (OTC) market, while XPT signifies the spot price of platinum in US dollars, also based on the trading activities within the same market. Bloomberg provided daily closing prices for XAU and XPT from January 1987 through January 2019, as seen in Fig. 13.

Table 2 presents the statistical attributes of the precious metals' spot prices. Both datasets exhibit positive skewness, with the platinum dataset showing a higher level of fluctuation within this time frame. A correlation test conducted on these two datasets yielded an outcome of 83%, signifying that the data maintains a consistent correlation for the span of 32 years. In the subsequent section, we will delve into the joint movement of the precious metals and their multifractal properties.

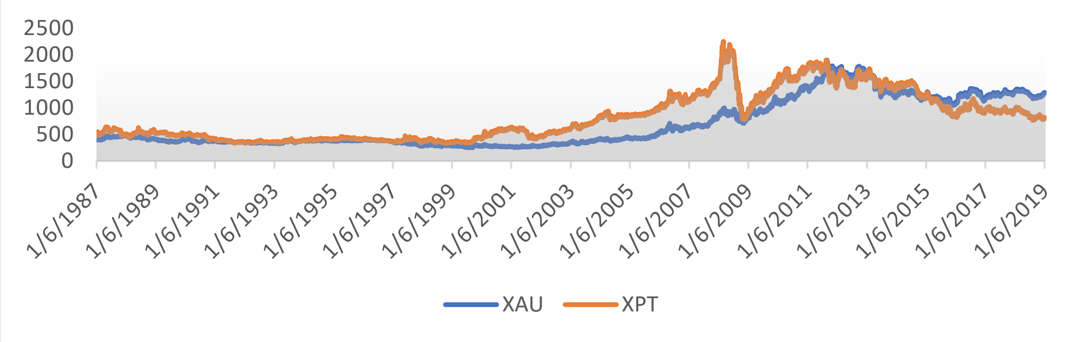

Figure 13. Spot prices of Gold and the spot price of Platinum.

Table 2. *Descriptive Statistics of Spot Prices of Precious Metals*

	Mean	Median	Std. Dev.	Skewness	Kurtosis
XAU	692.62	417.25	448.082	0.847233	-0.77595
XPT	830.05	637.50	454.7341	0.770928	-0.55472

2.2.2 Methodology

We utilized two distinct analytical tools, MF-X-DMA, and wavelet coherence analysis, to delve into the dynamic association between the prices of gold and platinum. By using a variety of methods, we were able to better comprehend the dynamic ties and interdependencies between these two valuable metals. The multifractal time-domain technique, MF-X-DMA, enables the identification of broad trends and dynamics by capturing long-range correlations and self-similarity in time series data. Conversely, wavelet coherence analysis, a frequency-domain method, inspects the coherence and phase correlations between time series across different frequency bands, offering insights into short- and medium-term dynamics.

Despite MF-X-DMA and wavelet coherence analysis employing different mathematical notions, both methods aim to uncover underlying dependencies and patterns in time series data. We were able to identify parallels and differences in the short- and long-term patterns of gold and platinum prices by merging the results from both techniques. This integration aids in providing a more comprehensive and nuanced scrutiny of the interplay between the two metals.

2.2.2.1 Continuous Wavelet Transform (CWT)

For a long time, the wavelet transform has been widely employed in the study of fractals and multifractals (Jiang, Gao, et al., 2017), (Jiang, Yang, et al., 2017), (Gencay, 2002). We specifically employ the Continuous Wavelet Transform (CWT) method, initially introduced by (Gencay, 2002), as a novel application of wavelet in finance. This method has been implemented by many researchers, as exemplified in (Aguiar-Conraria & Soares, 2014), (Vacha, 2013), (Yilmaz & Unal, 2016), (Oral & Unal, 2017), (Dogangun & Unal, 2019). There are two types of wavelet methods: discrete wavelet transforms and continuous wavelet transforms. The primary distinction between the CWT and discrete wavelet transforms, such as the dwt and modwt, is the manner of discretization of the scale parameter. The CWT carries out scale discretization more minutely than the discrete wavelet transform (Zhou, 2012).

The finite size effect in multifractal analysis (Jiang et al., 2019), (Zhou, 2012), (Drod et al., 2009), (Bogachev et al., 2007), (Oświęcimka et al., 2020) can be mitigated through the use of the CWT. This is attributed to the CWT's scale-dependent nature that allows for the exploration of a signal at varying sizes without the constraints of a fixed window size. Applying the CWT to a time series enables us to inspect the local features of the signal across diverse scales, and acquire more accurate details about the multifractal behavior of the signal. The CWT, in particular, allows us to compute the wavelet transform modulus maxima (WTMM), or the wavelet transform modulus maxima at different scales. The WTMM method is often utilized when estimating the multifractal singularity spectrum, which elucidates the multifractal behavior of the signal. In summary, the CWT is a powerful tool for studying a signal's multifractal attributes since it can offer a scale-dependent analysis less influenced by the finite size effect.

Our main objective is to conduct a detailed time-frequency analysis, thus we opted for CWT over other wavelet approaches (The MathWorks, 2022). Wavelet transforms facilitate the localization of frequency decomposition and the creation of information about frequency components. Grinsted et al., (2004) demonstrated that CWT outperforms other methods for detecting the evolution of signal frequency across the period of the signal and comparing the spectrum to the spectra of other signals. As a result, it is more widely utilized for feature extraction to see the findings in a more straightforward style (Oral & Unal, 2019). When using wavelet analysis to extract components, the Morlet wavelet (with ω =6) is an excellent choice since it provides a nice balance of temporal and frequency localisation.

A wavelet function is defined as follows:

$$\psi_0(n) = \pi^{-1/4} e^{i\omega_0 n} e^{-1/2n^2}, \tag{2.1}$$

where ω_o is frequency and n is time.

CWT follows the following form in Eq.(2.2)

$$W_x^{\psi}(\tau, s) = \langle X, \twoheadrightarrow \psi(s, \tau) \rangle = \frac{1}{\sqrt{s}} \int_{-\infty}^{+\infty} X(t)\, \psi^*(\frac{t-\tau}{s}) dt, \tag{2.2}$$

where * denotes complex conjugate. Wavelet transforms, often known as the mother wavelet, act as a band-pass filter. The rationale behind employing CWT to time series data lies in its ability to break down and subsequently reconstruct the data.

2.2.2.1.1 The Cross Wavelet Transform

According to Torrence and Compo (Torrence & Compo, 1998), the cross wavelet transform (XWT) of two time series, x_n and y_n, is denoted as $W^{XY}(u, s) = W^{X}(u, s)W^{Y*}(u, s)$. In this context, '*u*' symbolizes the positional index while 's' is representative of the scale. The cross wavelet power, which depicts the local covariance of the time series at each scale, is defined as $|Wxy(u, s)|$.

2.2.2.1.2 Wavelet Coherence

Wavelet coherence is used to find areas of co-movement between two time series in the time-frequency domain. P.J. Webster, (1999) construct the squared wavelet coherence coefficient as follows:

$$R_S^2(u,s) = \frac{|S(s^{-1}W_{xy}(u,s)|^2}{S(s^{-1}|W_x(u,s)|^2)S(s^{-1}|W_y(u,s)|^2)}, \tag{2.3}$$

S denotes the smoothing operator. The coefficient values will be between 0 and 1. When the value approaches 1 (zero), it implies a strong (weak) connection.

2.2.2.1.3 Phase Angle

The difference in the phase is calculated as

$$\psi_{xy}(\mathrm{u, s}) = tan^{-1}\left(\frac{I\{S((s^{-1}W_{xy}(u,s)))\}}{R\{S((s^{-1}W_{xy}(u,s)))\}}\right), \psi_{xy} \in [-\pi,\ \pi], \tag{2.4}$$

where I and R indicate the imaginary and real sections of the power spectrum, respectively.

2.2.2.1.4 The Cone of Influence

Given that the wavelet isn't entirely localized temporally, the CWT manifests edge artifacts. Due to discontinuity, the wavelet power falls to e^{-2} at the boundaries. This difficulty can be solved by padding the time series with a sufficient amount of zeroes. However, the introduction of a cone of influence (COI) proves to be a more effective solution. Grinsted et al., (2004) suggest that it is crucial to consider this, considering its impact on the boundaries.

2.2.2.2 MF-DFA and MF-X-DMA

The MF-DFA, a mathematical approach, is typically applied for scrutinizing complex data sets, most commonly in the fields of physics and environmental science. Castro E Silva & Moreira, (1997) originally proposed this technique in 1997 for identifying multi-affine fractal exponents. The method entails segmenting a time series into many segments of varied lengths and calculating the variation of each after the trend is removed. As shown by Weber & Talkner (2001), this approach has been used across various scenarios, including climate data analysis spanning days to decades. The MF-DFA method has proven effective for characterizing the scaling behavior of intricate systems and understanding their fundamental dynamics. In this study, we used Kantelhardt et al.'s, (2002) MF-DFA approach and Ihlen's (2012) Matlab tools in the execution of MF-DFA, as demonstrated in (Dogangun & Unal, 2019).

MF-DFA and MF-X-DMA can be used to investigate long-range correlations and multifractal characteristics in non-stationary time series. MF-X-DFA and MF-X-DMA are MF-DCCA extensions; the former is based on DFA, while the latter is based on DMA. The goal of multifractal detrended cross-correlation analysis is to investigate the multifractal character of long-range power-law cross-correlations between two non-stationary time series. "The main difference between MF-X-DFA and MF-X-DMA is that the latter uses a local moving average as the trend function" (Jiang & Zhou, 2011). When X(t)=Y(t), the DFA method becomes a special instance of the DCCA method. This circumstance reduces MF-X-DFA to MF-DFA and MF-X-DMA to MF-DMA.

Furthermore, existing literature demonstrates that MF-X-DMA can provide improved outcomes in the presence of trends and exhibit a higher degree of robustness. This approach generates more effective power-law scaling relationships and handles larger time scales than MF-DFA (Ghazani & Khosravi, 2020).

The MF-X-DMA is described in full below:

To begin with, consider *x(i)* and *y(i)* as stable time series of identical length *N*, with *i* representing the numbers *1, 2, …, N*. Presume that these two series have a mean of zero and that *X(i)* and *Y(i)* represent the cumulative sums of *x(i)* and *y(i)*, respectively.

Subsequently, the moving average function of *X* and *Y* is outlined as $\tilde{Z}(t)$ for a particular size, n.

$$\tilde{Z}(\mathrm{t})=\frac{1}{s}\sum_{k=-\lfloor(s-1)\theta\rfloor}^{\lceil(s-1)(1-\theta)\rceil} Z(t-k), \qquad (2.5)$$

In this context, θ represents a positional parameter which varies from 0 to 1. The symbols ⌊g⌋ and ⌈g⌉ correspond to the greatest integer that does not surpass g and the least integer that is not below g, respectively. As Zhou indicated, "the moving average function accounts for ⌈(s-1)(1-θ)⌉ data points in the past and ⌊(s-1) θ ⌋ points in the future."

There are three distinct scenarios concerning θ: when θ equals 0, it corresponds with the backward moving average, and $\tilde{Z}$(t) is computed based on all previous n-1 data points. If θ equals 0.5, it refers to the centered moving average, where Z(t) is calculated from an equal number of past and future data points. Finally, when θ equals 1, it lines up with the forward moving average, and $\tilde{Z}$(t) is determined based on all future s-1 data points (G. J. Wang & Xie, 2013).

In the third phase, we remove possible trends in the time series by deducting the moving average function $\tilde{Z}$(i) from Z(i). Consequently, we acquire the cross-correlation residual series ε(i) through the following method:

$$\varepsilon(i) = [X(i) - \tilde{X}(i)][Y(i) - \tilde{Y}(i)],$$

$$\text{where } s\text{-}\lfloor(s-1)\theta\rfloor \leq i \leq N - \lfloor(s-1)\theta\rfloor. \qquad (2.6)$$

Following that, the residual series ε(i) is partitioned into Nn=⌊N/s-1⌋ non-overlapping sections of uniform length s. For each unique non-overlapping section v, εv(i) corresponds to εv(l+i) for 1≤ i ≤s, where l=(v-1)n and 1≤ v ≤Ns. The cross-correlation variance for every segment is subsequently calculated as specified in Equation (2.7).

$$F(s,v) = \frac{1}{s}\sum_{i=1}^{s} \varepsilon_v(i). \qquad (2.7)$$

The qth order cross-correlation (or fluctuation function) is calculated in the fifth step by averaging across all segments

$$F_{xy}(q,s) = \{\frac{1}{N_s}\sum_{v=1}^{N_s} |F(s,v)|^{q/2}\}^{1/q}, \tag{2.8}$$

when q≠0 and

$$F_{xy}(0,s) = \exp\{\frac{1}{2N_s}\sum_{v=1}^{N_s} \ln|F(s,v)|\}. \tag{2.9}$$

In the concluding stage, the log-log depiction of Fxy(q,s) gives rise to the scaling connection of the fluctuation function as illustrated in Equation (2.10). If the two time series showcase a long-range power-law cross-correlation, the fluctuation function will grow as a power-law for larger values of n.

$$F_{xy}(q,s) \sim s^{h_{xy}(q)}. \tag{2.10}$$

The scaling exponent *hxy (q)* is proportional to q. This implies that *hxy (q)* > 0.5 indicates persistent (positive) cross-correlation between the two time series, implying that if *x(i)* increases (falling), *y(i)* is likely to rise (fall). In general, *hxy (q)* = 0.5 indicates that there is no cross-correlation between the two time series, and changes in *x(i)* have no effect on *y(i)*. A *hxy (q)* of 0.5 indicates anti-persistent (negative) cross-correlation between the two time series, indicating that if *x(i)* increases (falling), *y(i)* is likely to rise (fall) (C. Xie et al., 2017).

Furthermore, the DCCA coefficient is used to calculate the cross-correlation between two time series. The coefficient is defined as the product of the detrended fluctuation functions $F_{DCCA}^2(2,s)$ and $F_{DFA\{xt\}}(2,s)$ of the two time series, as stated by Equation (2.11):

$$\rho_{DCCA} = \frac{F_{DCCA}^2(2,s)}{F_{DFA\{xt\}}(2,s)F_{DFA\{yt\}}(2,s)}\,, \tag{2.11}$$

Here, ρ_{DCCA} can range between -1 and 1. A value of -1 points to a perfect anti cross-correlation between the two time series. On the other hand, a value of 1 signifies total perfect cross-correlation, and ρ_{DCCA}=0 suggests that there is no cross-correlation (Zebende, 2011).

2.2.2.3 Renyi Exponent

Using the multifractal theory formula, we can also use the Renyi (multifractal scaling) exponent to establish the type of multifractality using Equation. (2.12)

$$\tau_{xy}(q) = qh_{xy}(q) - D_f, \tag{2.12}$$

where D_f denotes the fractal dimension of the multifractality's geometric base. D_f = 1 in the case of time series analysis.$\tau_{xy}(q)$ characterizes the scaling behavior; if $\tau_{xy}(q)$ shows linearity with q, the behavior is monofractal. The scaling behavior, on the other hand, is multifractal. This suggests that with an increase in nonlinearity, multifractality thrives.

Furthermore, the singularity spectrum $f_{xy}(\alpha)$ of the Hölder exponent α_{xy} is a widely used indication for evaluating the multifractality of two time series.The multifractal spectrum $f_{xy}(\alpha)$ is described by the Legendre transform of $\tau_{xy}(q)$ as stated in Equation (2.13) (Kim et al., 2011).

$$f_{xy}(\alpha) = \alpha q - \tau_{xy}(q),\ \alpha = \frac{d\tau_{xy}(q)}{dq}. \tag{2.13}$$

2.3 Empirical Results

2.3.1 Wavelet Coherence

The wavelet coherence of gold and platinum may be found in Figure 14. One can tell that almost at all times, gold is the leading element of the couple since the arrows are pointing right. The only exception may be found in the 2048-day period from 2001 to 2009 which is not statistically significant. The series are moving in coherence from September 2, 2002, to May 4, 2010, between 256 and 512-day period. Long-term and short-term co-movement tendencies have risen in recent years compared to previous years.

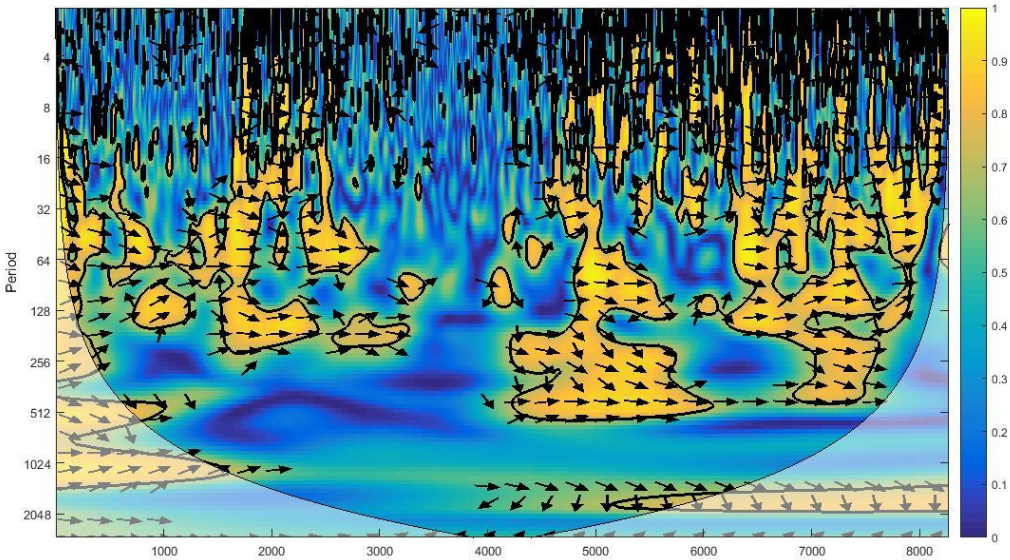

Figure 14. Wavelet Coherence of Gold and Platinum

2.3.2 The Cross-correlation and Multifractality

Using multiple wavelet coherence, we conduct a cross-correlation analysis. We assign window sizes ranging from 8 to 4096 (2n where n=3, …, 12), taking into account that wavelet analysis often deals with powers of 2, and we set the *q*-order from -9 to 9.

H(q) does not depend on q for monofractal time series, which have a constant exponent across all time scales. However, h(q) changes as q changes for multifractal time series.

Because of the different scaling of smaller and bigger variations, h(q) is highly dependent on q. When q is positive, h(q) describes the scaling behavior of segments with higher variations. In contrast, the scaling exponent h(q) describes the scaling behavior of segments with fewer variations for negative q values (Lu et al., 2013).

The log-log fluctuation function of *Fxy(q, s)* concerning the time scale s is demonstrated in Fig. 15. The value of the fluctuation function decreases at the same scale *s* as the *q* value diminishes. This implies that fluctuation increases consistently with *q*. Additionally, it's more straightforward to note that fluctuation values increase linearly with *s*. Considering that the plot is a log-log plot, the intensity of fluctuation dramatically increases with positive *q* compared to negative *q* values as the scale value s increases. It indicates that the fluctuation becomes weaker as the q-order decreases. Thus, the multifractal cross-correlation between gold and platinum is observed across all scales.

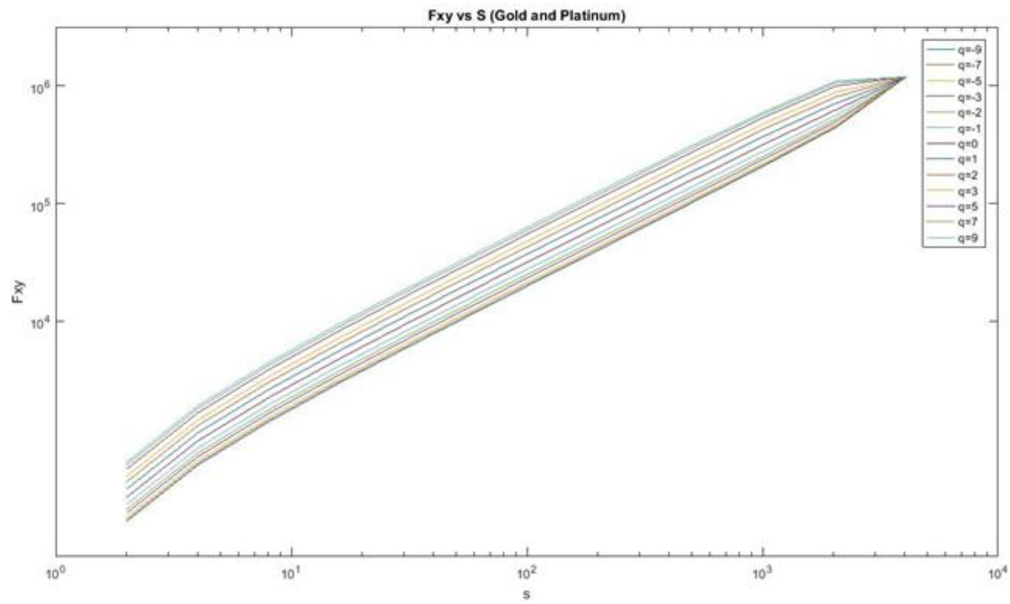

Figure 15. The log-log plot of fluctuation function Fxy(q,s) with respect to time scale of s (from 8 to 4096 with the power of 2 steps)

As seen in Fig. 16 when the scale intervals are decreased to 2 steps each, there is little fluctuation at the higher scales and stronger with positive order of q. Fig. 17 plots the same graph for a highly correlated time interval between 2001 and 2009.

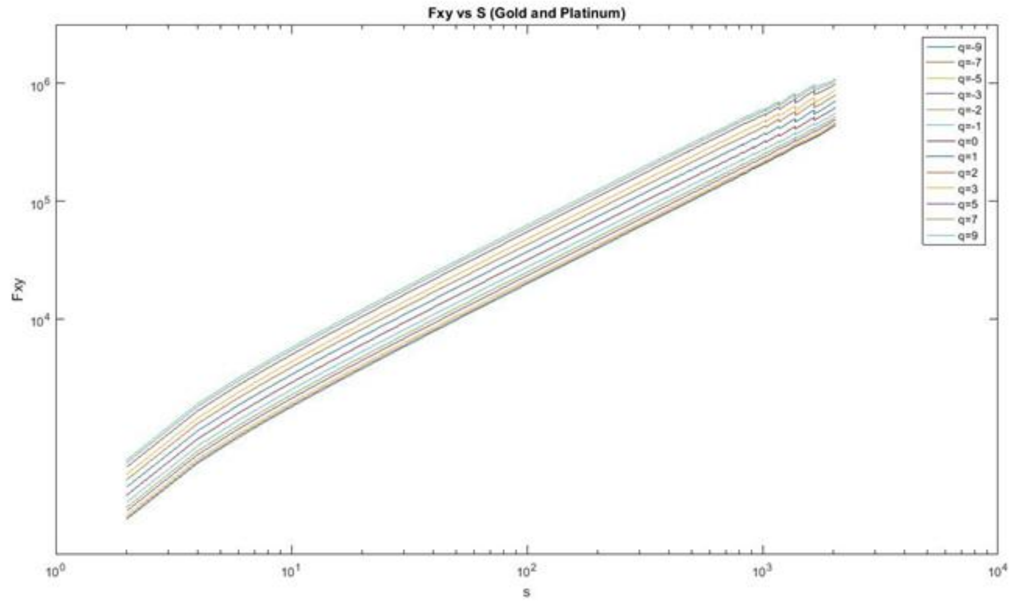

Figure 16. The log-log plot of fluctuation function Fxy(q,s) with respect to the time scale of s (from 8 to 2048 with steps of 2)

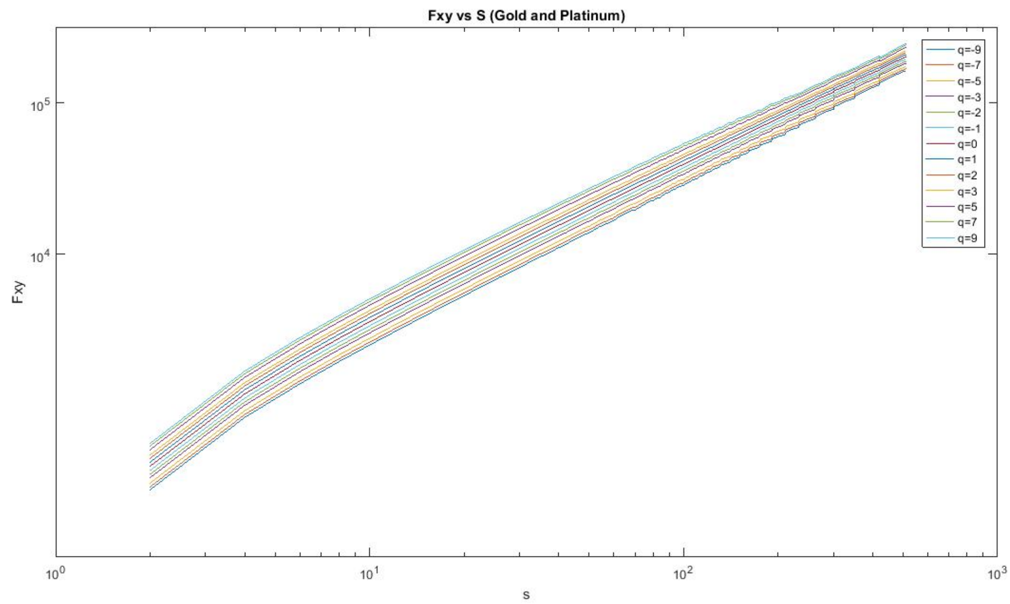

Figure 17. The log-log plot of fluctuation function Fxy(q,s) of Highly correlated time interval with respect to the time scale of s (from 8 to 512 with steps of 2) between 2001 and 2009

When the F vs s graph is plotted with a Theta value of 0.5, the graph undergoes a significant change as depicted in Fig. 18. Up to a scale of 32, F values are mostly constant for all q values. After that, F values begin to rise except for q values of -9, -7, and -5, which decrease up to a scale value of 128. Fig. 19 illustrates the same graph over the same time span with a smaller alteration in the values of scale, s= 2, 4, 6, 8,…. When the q values are negative, the fluctuation between steps intensifies. Nevertheless, it's important to note that the fluctuations at each scale do not intersect with different q-order values.

When examining the same analysis at theta=0.5 for the highly correlated time interval, the constant fluctuation behavior is similarly observed up to scale 32 as shown in Fig. 20. However, the fluctuation is comparatively weaker, especially for negative q-order values, when compared to real data.

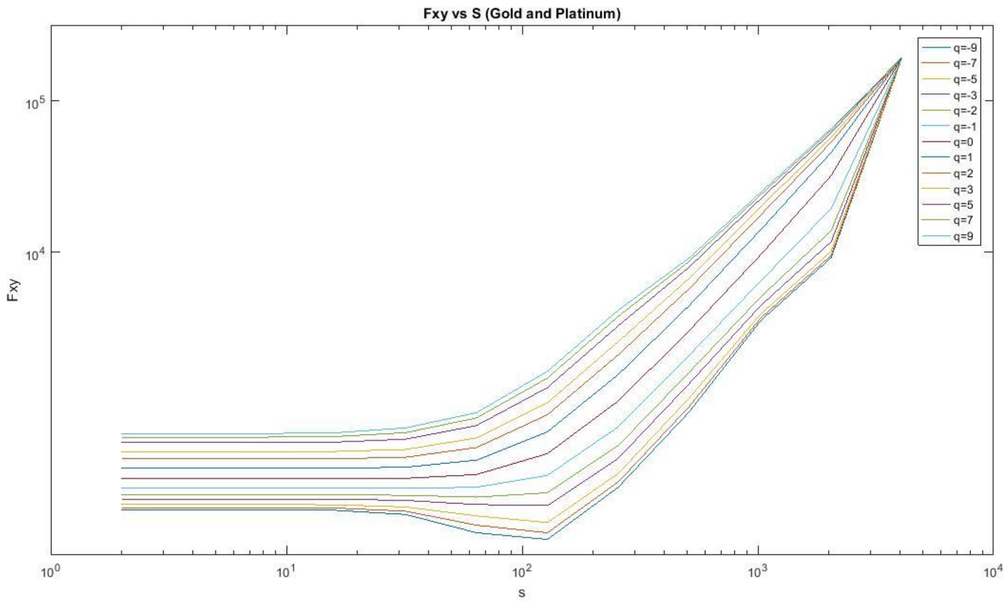

Figure 18. The log-log plot of fluctuation function Fxy(q,s) of Highly correlated time interval with respect to the time scale of s (from 8 to 4096 with power of 2 steps) Theta=0.5

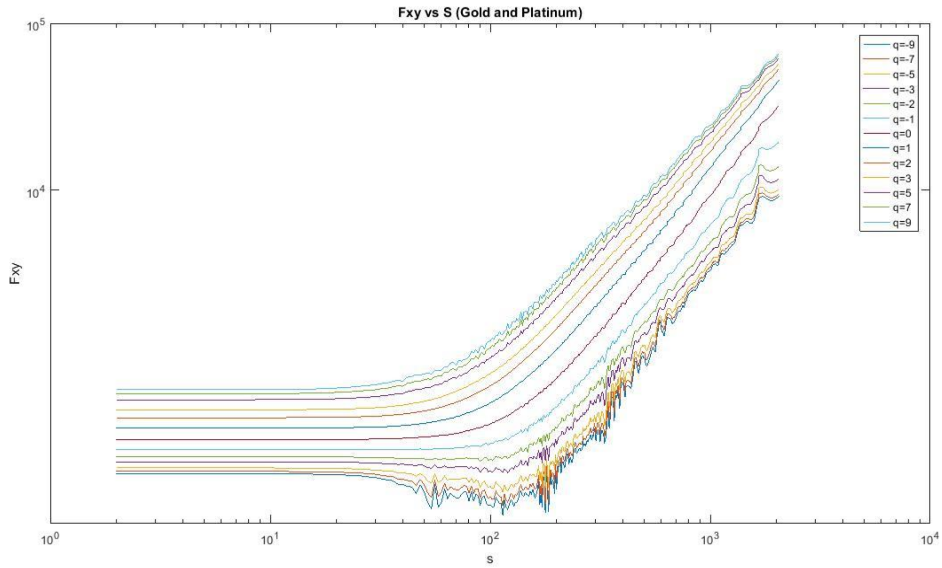

Figure 19. The log-log plot of fluctuation function Fxy(q,s) with respect to the time scale of s (from 8 to 2048 with steps of 2) Theta=0.5

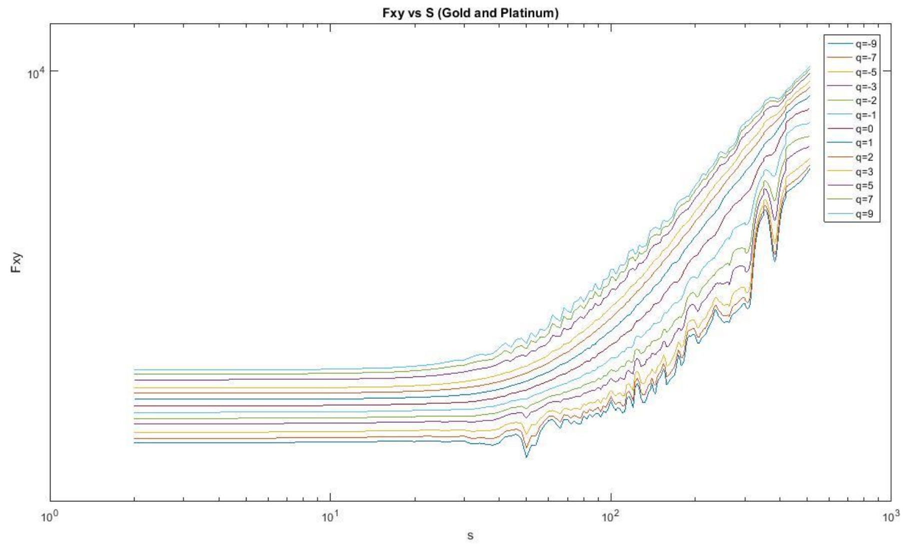

Figure 20. The log-log plot of fluctuation function Fxy(q,s) of Highly correlated time interval with respect to the time scale of s (from 8 to 512 with steps of 2) between 2010 and 2016 Theta=0.5

2.3.3 The DCCA and The Hurst Exponents

The DCCA coefficient serves as an additional metric for evaluating the cross-correlation relationship between two time series. As illustrated in Fig 21, all ρ_{DCCA}

values exceed 0.95 and approach 1 as the scale enlarges. This aligns with the Epps effect, suggesting that correlations between two time series usually intensify with escalating time scale (Epps, 1979), (Bence Toth; Janos Kertesz, 2009). From an economic perspective, it can be argued that the relationship between gold and platinum is in sync at all times. Simultaneously, this synchronized movement strengthens over extended periods. This could be linked to the gradual depletion of the noises from gold and platinum.

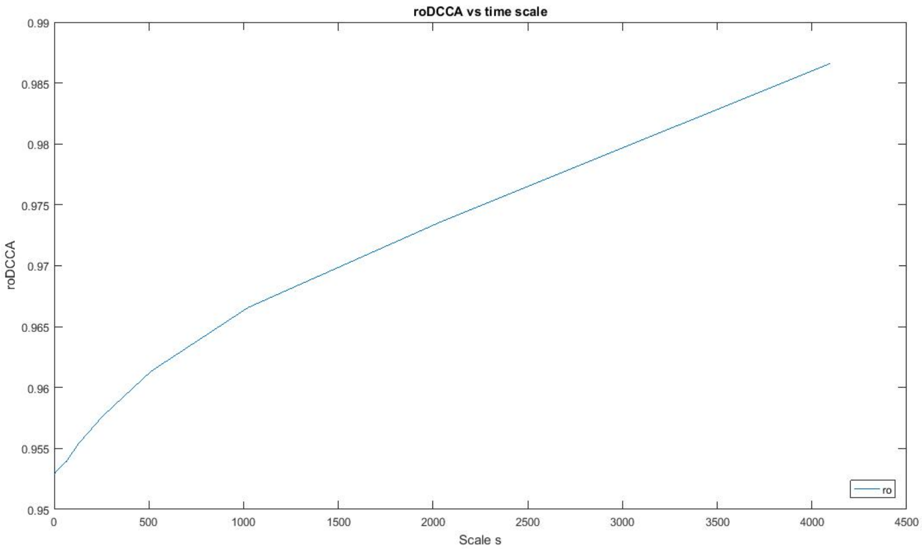

Figure 21. The DCCA coefficients with respect to time scale s (with the power of 2 steps (s=2,4,8,16,…))

When we analyze the data with scale values that are increasing 2 step each time, the graph becomes as in Fig. 22.

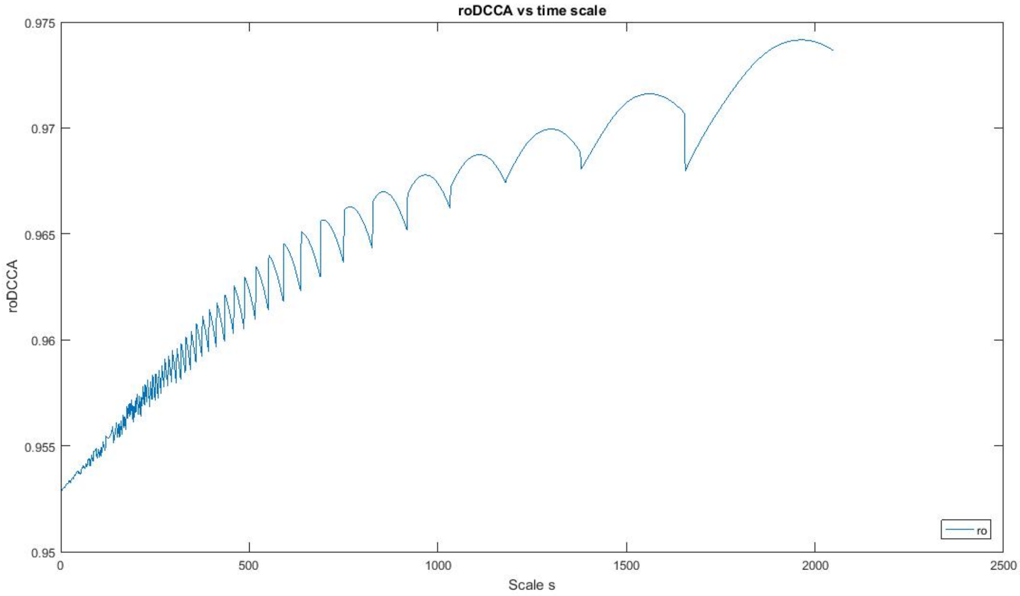

Figure 22. The DCCA coefficients with respect to time scale s (with steps of 2 (s=2,4,6,8,10,12,14,16,…))

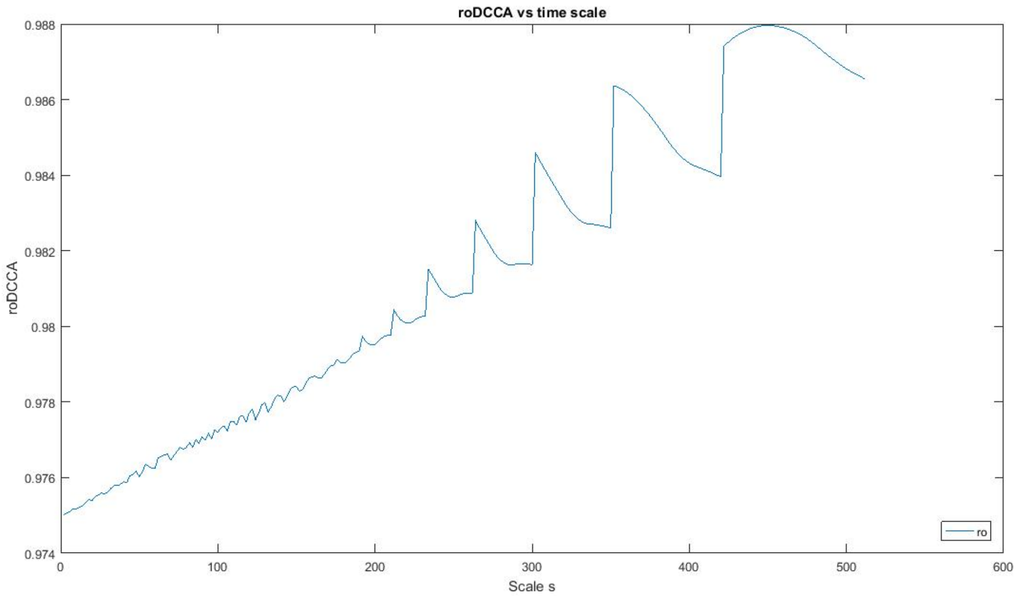

Figure 23. The DCCA coefficients from the highly correlated area from 2010 to 2016 with respect to time scale s (with steps of 2 (s=2,4,6,8,10,12,14,16, …))

Gold and platinum cross-correlations are multifractal, and $h_{gp}(q)$ declines with the order of q, as illustrated in Fig. 24. Accordingly, gold and platinum cross-correlation exhibits a multifractal behavior. As the Hurst exponent value swells, it manifests more evident slow-evolving fluctuations (Bence Toth; Janos Kertesz, 2009). Given that all Hurst exponent values surpass 1, the cross-correlation shows stronger persistence in large fluctuations than in small ones. This points to the commodities possessing a complete long memory, with persistent fluctuations. In other words, for large fluctuations, when gold or platinum rises (falls), the other likely follows suit. Moreover, the Hurst exponent values for platinum are higher than those for gold, suggesting more enduring fluctuations in platinum's autocorrelation than in gold's. Podobnik et al. demonstrate that the Hurst exponents for two distinct ARFIMA processes with order q=2 are equal to the cross-correlation Hurst exponents. Using the p-model, Zhou establishes two binomial measures and reveals that $h_{gp}(q)$ equals the arithmetic average of $h_{gg}(q)$ and $h_{pp}(q)$, expressed as $h_{qp}'(q)$. While Hurst exponents diverge significantly from one another when the q order is negative, they tend to converge when q is positive. However, Hurst exponents were found to be closely related when considering the highly correlated section. The cross-correlation's Hurst exponent is marginally lower than the computed value but still adequate to highlight the aforementioned equality. When the data is extracted from a highly correlated time series, the q-order transition in relation to the Generalized Hurst Exponent appears smoother, as presented in Fig. 25.

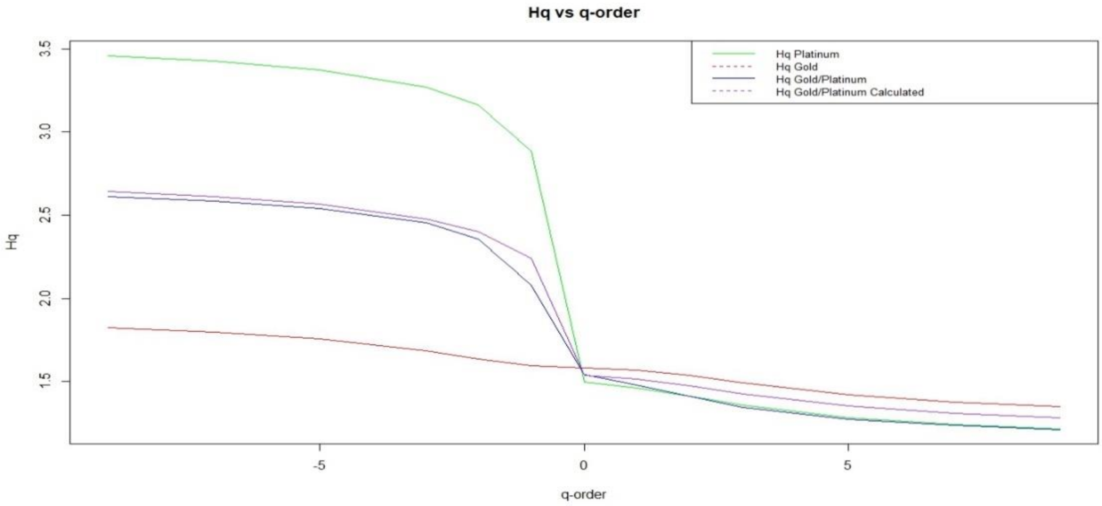

Figure 24. Generalized Hurst exponents hgp(q) vs order q

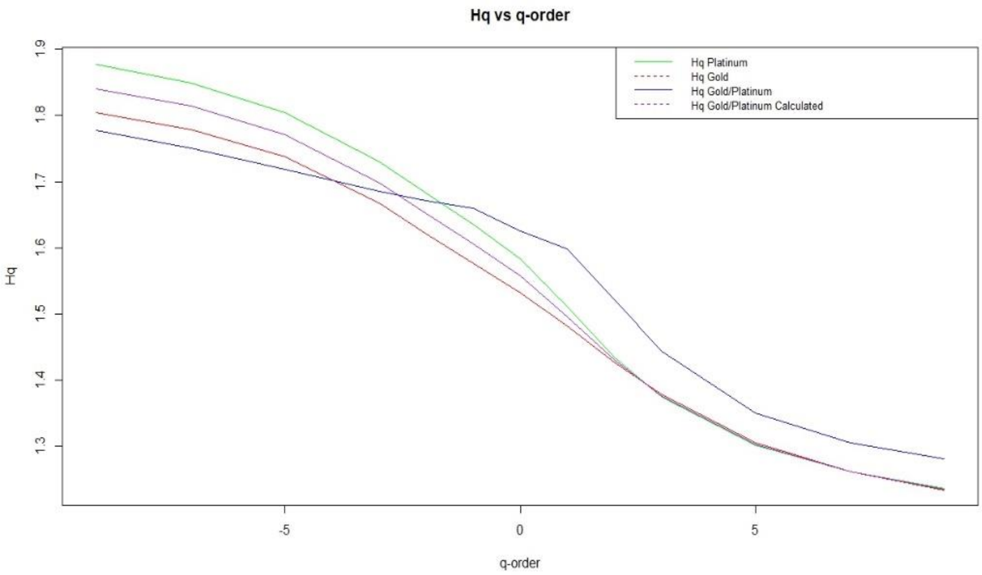

Figure 25. Generalized Hurst exponents hgp(q) vs order q from the highly correlated time interval (between 2010 to 2016)

2.3.4 The Renyi Exponents

To validate our findings on multifractal behavior, we plot the Renyi exponents of gold, platinum, and the gold/platinum ratio in Fig. 26. When the order of q is positive, the

Renyi exponents coincide. However, for negative *q*-order values, the Renyi exponent of gold is highest and that of platinum is lowest. The nonlinearity of the Renyi exponents with the order of *q* indicates a multifractal cross-correlation between gold, platinum, and the gold/platinum ratio. When we consider highly correlated time series, the Renyi exponents were closely aligned, even for negative *q*-order values, as illustrated in Fig. 27. Both outcomes corroborate our earlier discoveries.

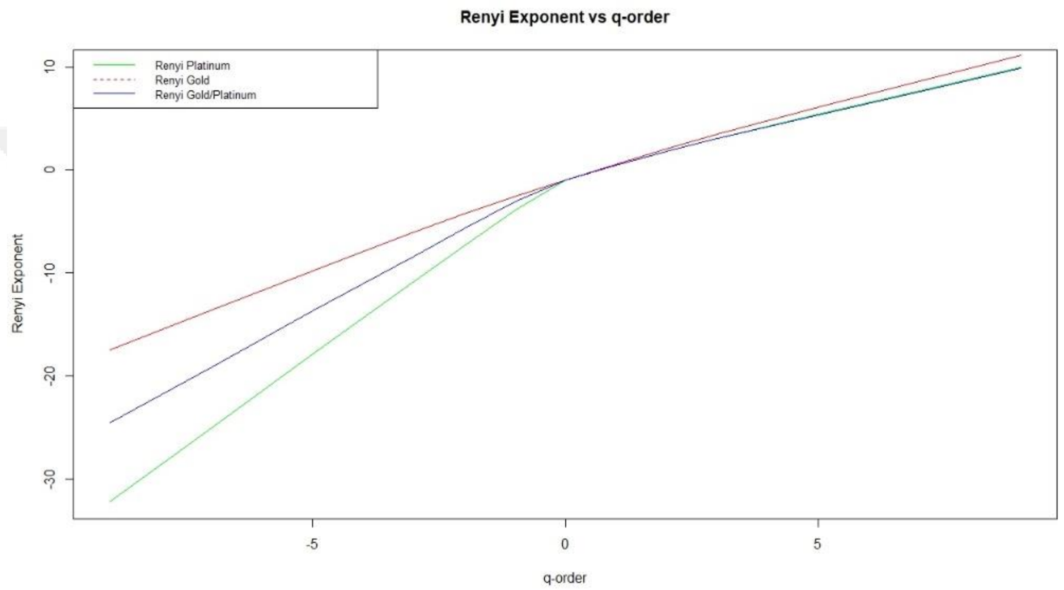

Figure 26. Renyi Exponent vs q-order

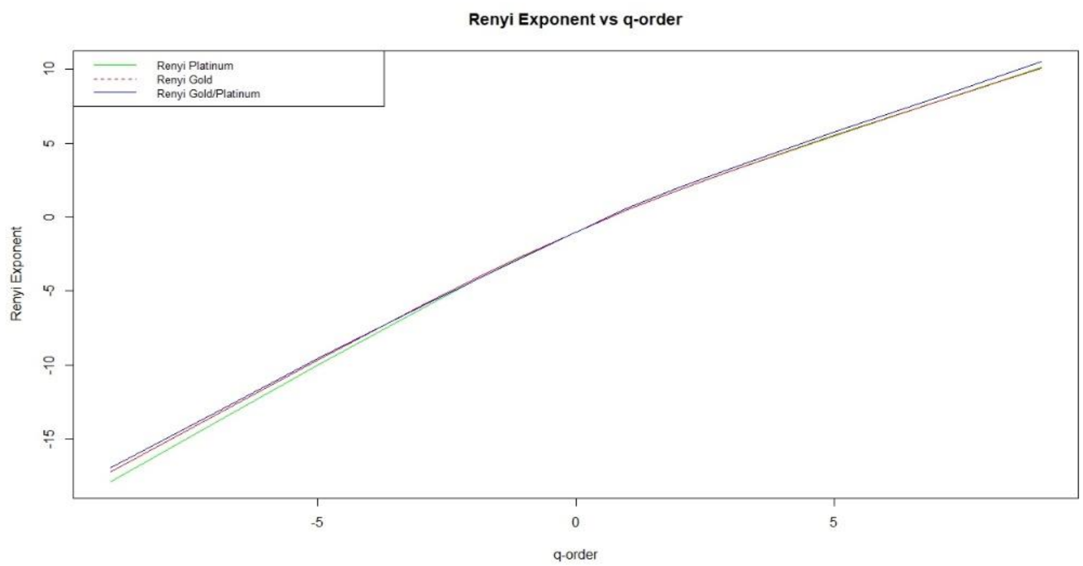

Figure 27. Renyi Exponent vs q-order (between 2010 and 2016)

2.4 Comparison of The Correlated and The Uncorrelated Time Periods

In this section, the author used the inversed CWT to extract the frequency of the price data presented in Fig.28. We detected the correlated and the uncorrelated time periods of gold and platinum spot prices by wavelet coherence which is shown in Fig. 29-30. Since the inversed CWT method has already pointed out the significant and insignificant time periods, we eliminated the shuffling and rolling window approach (Zhou, 2009).

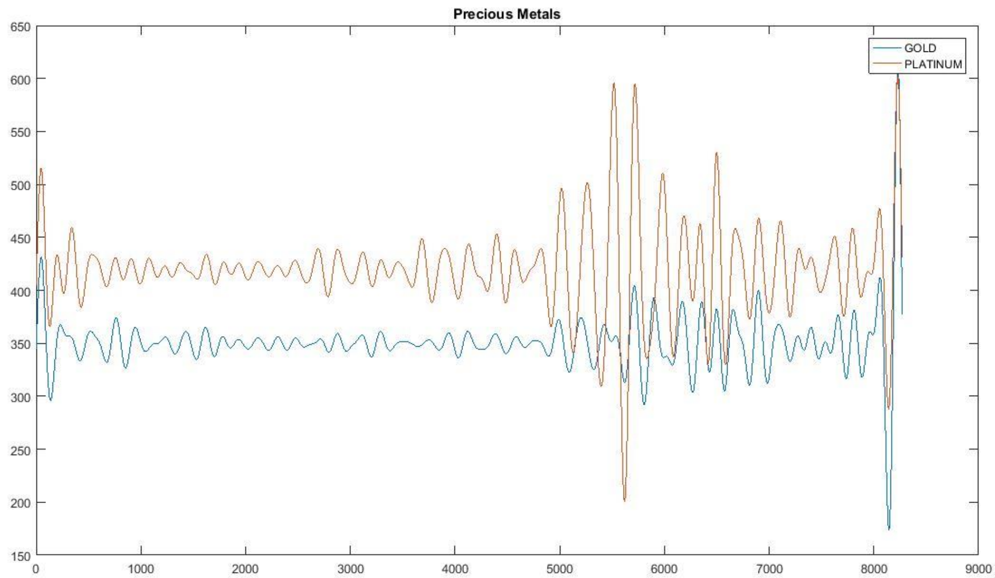

Figure 28. XAU and XPT Inversed Price Data at Scale 256

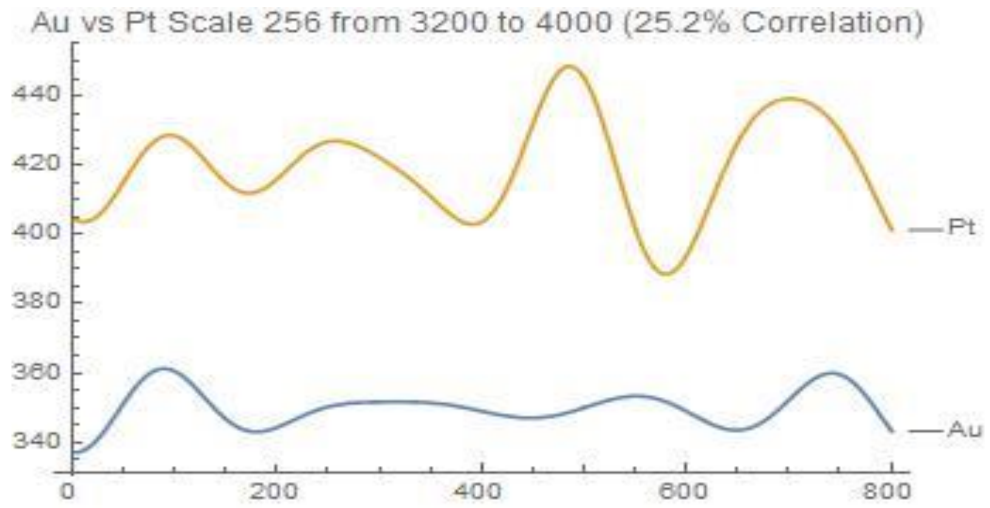

Figure 29. The Low Correlated XAU and XPT Inversed Price Data at Scale 256 between 20.7.1999 and 13.8.2002

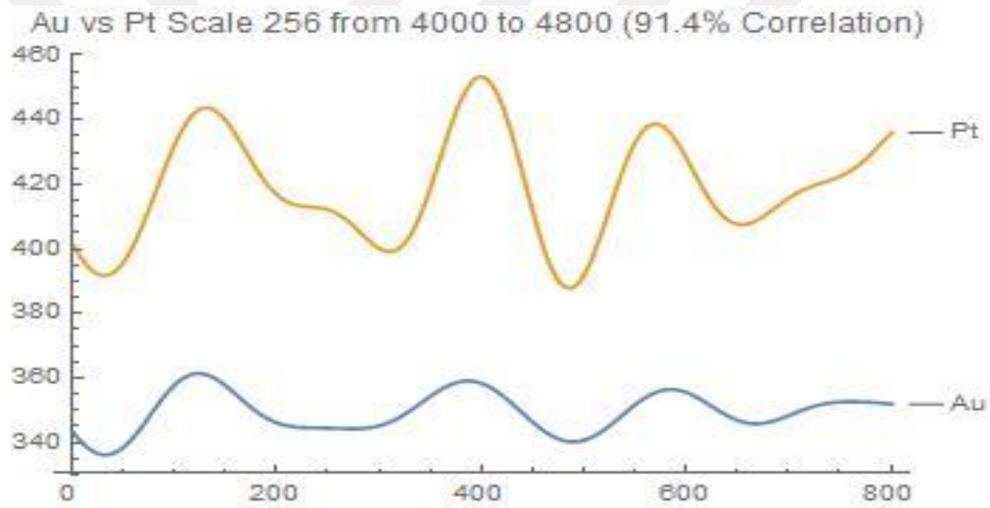

Figure 30. The High Correlated XAU and XPT Inversed Price Data at Scale 256 between 13.8.2002 and 06.9.2005

The low correlated area is equal to 800 data points and occurred between July, 20th 1999 and August, 13th 2002, at scale 256 which has 0.252 coherency. The following 800 data points are utilized as the highly correlated time period between August, 13th 2002 and September, 6th 2005; the coherency of the examined time period is 0.914 at scale of 256.

The DCCA coefficients of the inversed platinum and the inversed gold prices are greater than 0.99 and get closer to 1 for both low-correlated and high-correlated time periods. This research shows that even if the two time series have low correlation, they can exhibit long-term power law cross-correlation.

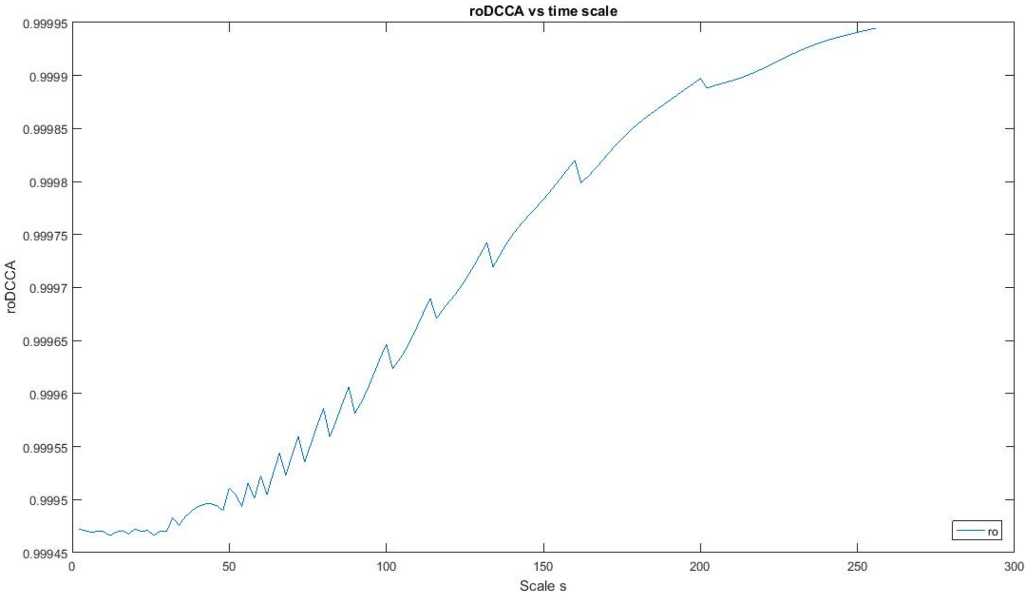

Figure 31. The DCCA coefficient of the inversed gold and platinum in the low correlated time period at scale 256 with steps of 2

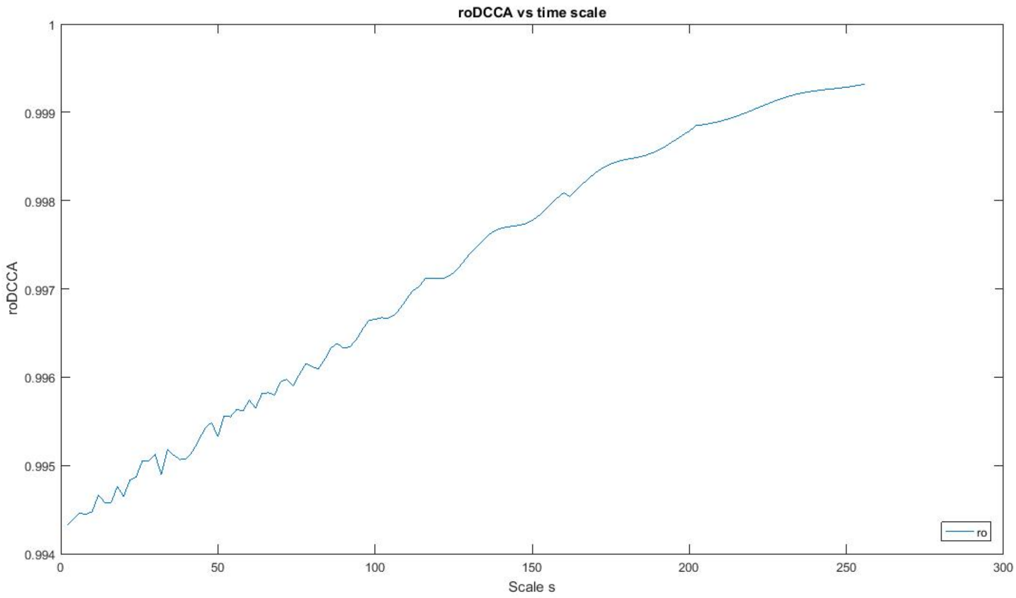

Figure 32. The DCCA coefficient of the inversed gold and platinum in the high correlated time period at scale 256 with steps of 2

To delve out the efficiency of the methods, both the low correlated and the highly correlated time periods were analyzed with the MF-DFA and the MF-X-DMA. Firstly, we conducted a MF-DFA. The outcomes indicate that both data exhibit multifractal behavior, indicating high volatility and unpredictability in the market, regardless of whether the correlation is low or high. Specifically, the general Hurst exponents of both the inversed gold prices and inversed platinum prices are greater than 1, suggesting strong long-term memory and persistence in the data. During the low correlated time period, the Hurst exponent of the inversed gold prices and inversed platinum prices are found to be 1.3636 and 1.3705, respectively. In the highly correlated time period, the Hurst exponent of the inversed gold and inversed platinum prices are found to be 1.4641 and 1.4377, respectively. These findings have significant implications for financial risk management and trading techniques. They imply that inversed gold and platinum prices are extremely complex and impossible to forecast over lengthy time periods.

Secondly, the MF-X-DMA is employed for detecting the fluctuation functions of the inversed precious metal prices, as shown in Fig. 33-34. Nevertheless, when θ equals 0.5, the fluctuation functions log-log plots' of both high and low-correlated time intervals displays a different projection.

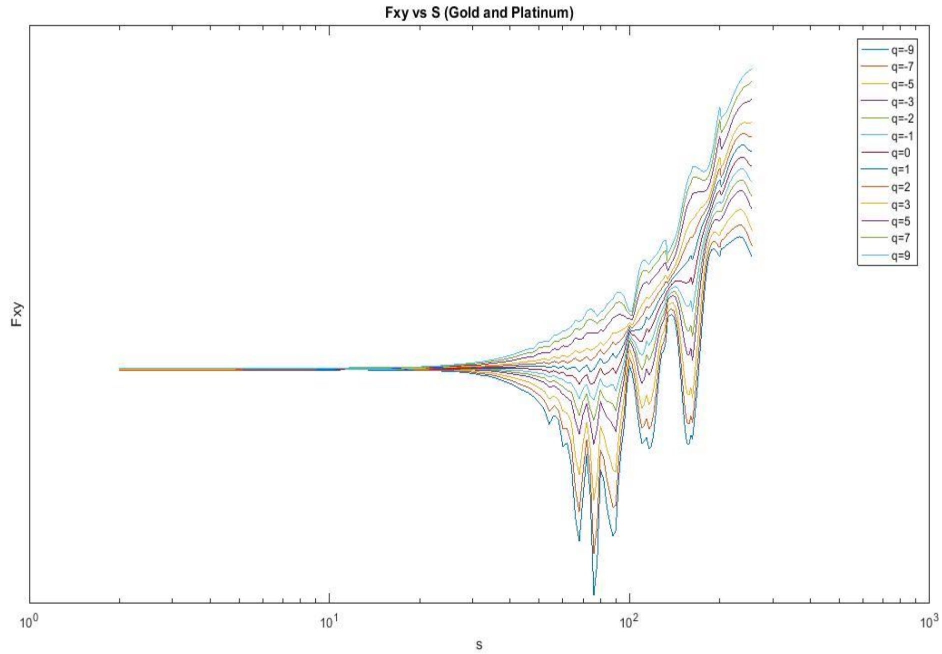

Figure 33. The log-log plot of fluctuation function Fxy(q,s) of low-correlated time interval with respect to the time scale of 256 (with the power of 2 steps) Theta=0.5

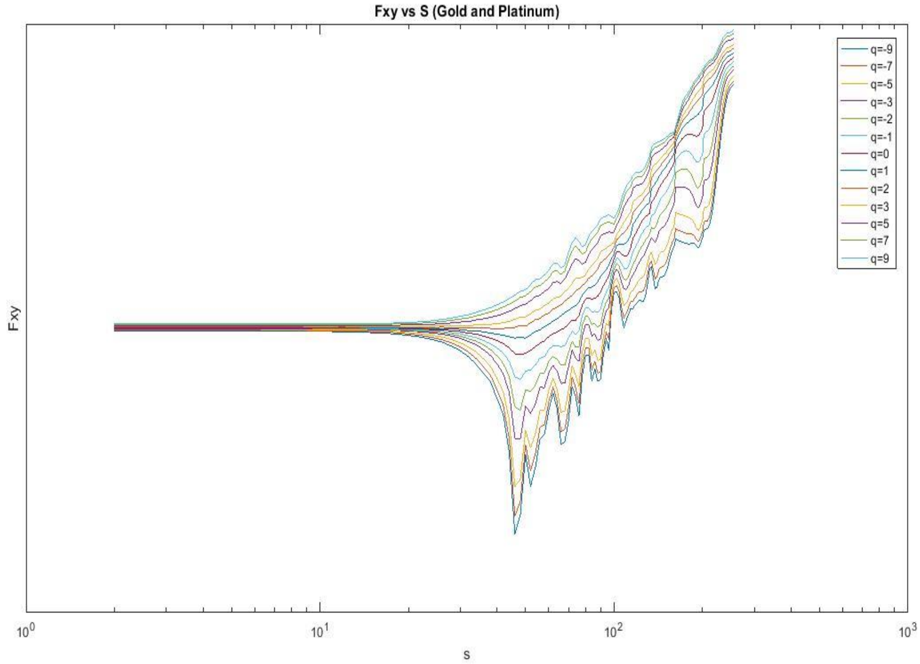

Figure 34. The log-log plot of fluctuation function Fxy(q,s) of high-correlated time interval with respect to the time scale of 256 (with the power of 2 steps) Theta=0.5

As demonstrated by C. Xie and colleagues, the cross-correlation analysis indicates that negative q values correspond to small fluctuations, yet these fluctuations become more pronounced rather than diminishing, as depicted in Fig.34. Thus, when the time series exhibits high correlation, MF-X-DMA offers superior results compared to MF-DFA. High correlation co-movement data is scrutinized more meticulously with MF-X-DMA with varying scale values. As a result, we can determine whether or not the time series displays significant changes and acquire a better grasp of the multifractal cross-correlations between the selected data sets.

2.5 Conclusion

In this study, we assess the effectiveness of the MF-X-DMA for multifractal time series exhibiting significant coherence during specific time periods. In the empirical procedure, we initially locate the areas exhibiting coherence at particular scales using a continuous wavelet transform. Subsequently, we employ various methods to reconfirm the multifractality of the precious metals' spot prices. The log-log plot of the fluctuation function confirms the presence of multifractal cross-correlation between gold and platinum at all scales in the cross-correlation investigation.

The DCCA coefficient and the Hurst exponent are used as a second approach. All DCCA coefficient values are above 0.95 and approach 1 as the scale increases, indicating a consistent correlation between gold and platinum, strengthening over longer periods. Looking at the Hurst exponent values, all values exceeding 1 imply that cross-correlation is more persistent for larger fluctuations. This shows that commodities have a long memory, with enduring swings. As a result, with considerable swings, an increase (or decrease) in gold or platinum results in an increase (or decrease) in the other. Furthermore, the larger Hurst exponent values for platinum indicate that its autocorrelation oscillations are more persistent than those of gold. Furthermore, we demonstrated that Renyi exponents are nonlinear with q's order, confirming the multifractal character of cross-correlation.

We used inversed CWT to extract the relevant frequency from the price data and identified the correlated and uncorrelated time periods for gold and platinum spot prices after finding the multifractality of the spot prices for gold and platinum. Given that the inversed CWT method already identified significant and insignificant time periods, we dispensed with the shuffling and rolling window approach.

The DCCA coefficients of the inversed platinum and gold prices inspected are greater than 0.99, moving closer to 1 for both low-correlated and high-correlated time periods. This finding demonstrates that even if the two time series are not highly correlated, long-term power-law cross-correlation can occur.

Finally, we present the MF-DFA and MF-X-DMA results for both low-correlated and high-correlated time series. The MF-X-DMA results confirm that even for time intervals with low correlation, long-term memory may be present. Despite the significant results of MF-DFA, the fluctuation function of the high-correlated time period exhibits a different behavior in MF-X-DMA, with stronger fluctuations for negative q values. The centered MF-X-DMA provides superior results than MF-DFA for high-correlated time series. In short, using co-movement time series, MF-X-DMA results can detect long-term memory more accurately. We conclude that WT is a powerful tool for extracting data for specific time and frequency intervals, enabling us to extract the most correlated time series, and that MF-X-DMA surpasses MF-DFA with outstanding results for the high-correlated time series.

In summing up, this research has rendered invaluable revelations regarding the multifractality of XAU and XPT spot prices by applying continuous wavelet transform and the MF-X-DMA. The outcomes unveiled a pronounced multifractal cross-correlation across all scales between the spot prices of gold and platinum. This understanding bears noteworthy economic and financial consequences as it can aid investors and financial analysts in diversifying their portfolios and managing risk more efficiently.

The indubitable long memory and sustained oscillations of the cross-correlation between the spot prices of gold and platinum also bear notable implications for commodities traders. This indicates that the prices of both commodities are not detached from one another, and that alterations in one may lead to predictable effects on the other. Traders can leverage this discernment to construct effective trading blueprints.

Furthermore, the DCCA coefficients of the inverted platinum and gold prices exceed 0.99 for both low- and high-correlated time periods, suggesting that even when the two commodities lack strong correlation, they may still exhibit long-term power law cross-correlation. This data could be of immense value to investors who aim to diversify their portfolios with assets that have a lower degree of correlation.

In essence, the integration of the CWT and the MF-X-DMA technique has shown efficacy in pinpointing long-term memory in co-movement time series. The revelations of this study could render valuable insights into the real interplay between the gold and platinum markets. This investigation furnishes fresh insights into the dynamics of gold and platinum markets, which can shape investment strategies and risk management practices.

3. Discussions

This multifaceted research inquiry has successfully amalgamated distinct methodologies to scrutinize the multifractal nature and cross-linkages of XAU and XPT spot prices. By employing continuous wavelet transform along with MF-X-DMA, we have derived crucial insights regarding the pronounced multifractal cross-correlation that exist across all scales between these two precious metals' prices. Parallelly, significant emphasis has been devoted to refining the Vector Fractionally Integrated Autoregressive Moving Average (V-FARIMA) modelling and forecasting, capitalizing on the deployment of multiple wavelet coherence of Hölder exponents for precious metal time series that have multifractal behavior.

The conclusions drawn from the MF-X-DMA scrutiny carry substantial economic connotations. They infer that fluctuations in the prices of gold and platinum are interdependent, offering traders predictive discernment that can aid in the formulation of efficacious trading blueprints. These discernments regarding cross-correlation persist even during periods of low correlation, underlining the possibility of long-term power law cross-correlation. Consequently, this investigation can supply pivotal information for investors seeking to augment their portfolios with assets exhibiting low correlation.

In a similar vein, the V-FARIMA modelling furnishes pivotal discernments. This investigation underscored three fundamental areas of concentration that bolster the accuracy of forecasting Hölder exponents of precious metal time series that have multifractal behavior when computed at associated time scales. This predictive stratagem unveiled a unique multifractal structure in precious metal price data, which is particularly vital during financially turbulent periods. Comprehending this multifractal structure facilitates enhanced forecasting of commodity price shifts, thereby assisting in the formulation of refined financial crisis prediction models.

Additionally, the use of Morlet Wavelet analysis detected coherent temporal intervals, and these interconnections were further scrutinized through the Wavelet Transform Coherence (WTC) methodology. The significant linkages discovered between gold and platinum prices across an array of frequencies and time frames bolster the concept of co-movement behaviour in the commodities markets. This understanding could enable informed trading decisions, efficacious strategies, and foster diversification within investor portfolios.

A detailed examination of the WTC outcomes of the Hölder exponents demonstrated significant uniformity at lower frequencies, hinting at persistent co-movement over elongated periods. This uniformity not only endorsed our preliminary observations of long-memory traits but also enhanced the reliability of our suggested forecasting approach. Essentially, the V-FARIMA model significantly upgrades the accuracy of forecasting the Hölder exponents of precious metal time series that have multifractal behavior when calculated at coherent time intervals.

Conversely, the deployment of ARIMA and VARIMA models led to less than satisfactory results. The capacity of the V-FARIMA model to encompass both long and short memory components showcases it as an essential instrument in accurately modelling the intricate dynamics of the multifractal time series, and thereby, a promising stratagem for successfully forecasting multifractal time series.

The fusion of the two distinct methodologies - MF-X-DMA and V-FARIMA - in this investigation presents a nuanced comprehension of precious metal markets. The outcomes furnish priceless discernments into the dynamics of gold and platinum markets, which could notably influence investment strategies and risk management practices, particularly in commodities trading.

Notwithstanding the potential of these approaches, it's crucial to acknowledge the requisite for computational power and expertise. These methodologies, although advanced and accurate, can be computationally demanding. However, for entities possessing the necessary computational capacity and expertise, these strategies could be transformative in terms of enhancing forecasting capabilities in precious metal markets, leading to improved investment decisions.

In conclusion, the investigation presents novel methodologies to comprehend and forecast price movements in the precious metal markets. The combination of Wavelet Coherency, MF-X-DMA and V-FARIMA offers a potent toolkit for both market analysis and forecasting, providing investors and analysts with a fresh perspective to decipher and navigate the complexities of the commodities market.

REFERENCES

Aguiar-Conraria, L., & Soares, M. J. (2011). The Continuous Wavelet Transform: A Primer. NIPE Working Paper. *Núcleo de Investigação Em Políticas Económicas, Universidade Do Minho, 16*, 1–43. http://www.economics-ejournal.org/economics/journalarticles/2011-16/references/@@export%5Cnhttp://www.eeg.uminho.pt/economia/nipe%0A*

Aguiar-Conraria, L., & Soares, M. J. (2014). The continuous wavelet transform: Moving beyond uni- and bivariate analysis. *Journal of Economic Surveys*, *28*(2), 344–375. https://doi.org/10.1111/joes.12012

Bence Toth; Janos Kertesz. (2009). The Epps effect revisited. *Quantitative Finance*, *9*(7), 1–23.

Bogachev, M. I., Eichner, J. F., & Bunde, A. (2007). Effect of nonlinear correlations on the statistics of return intervals in multifractal data sets. *Physical Review Letters*, *99*(24), 1–4. https://doi.org/10.1103/PhysRevLett.99.240601

Burrus, C. S., Gopinath, R. A., & Guo, H. (1998). Introduction to Wavelets and Wavelet Transforms: A Primer. In *Recherche*. http://www.amazon.com/Introduction-Wavelets-Wavelet-Transforms-Primer/dp/0134896009

Cao, G., Han, Y., Cui, W., & Guo, Y. (2014). Multifractal detrended cross-correlations between the CSI 300 index futures and the spot markets based on high-frequency data. *Physica A: Statistical Mechanics and Its Applications*, *414*, 308–320. https://doi.org/10.1016/J.PHYSA.2014.07.065

Castro E Silva, A., & Moreira, J. G. (1997). Roughness exponents to calculate multi-affine fractal exponents. *Physica A: Statistical Mechanics and Its Applications*, *235*(3–4), 327–333. https://doi.org/10.1016/S0378-4371(96)00357-3

Chow, G., Jacquier, E., Kritzman, M., Lowry, K., Chow, G., Jacquier, E., Kritzman, M., Lowry, K., Chow, G., Jacquier, E., Kritzman, M., & Lowry, K. (1999). Optimal Portfolios in Good Times and Bad. *Financial Analysts Journal*, *55:3*(65–73). https://doi.org/10.2469/faj.v55.n3.2273

Dai, M., Hou, J., & Ye, D. (2016). Multifractal detrended fluctuation analysis based on fractal fitting: The long-range correlation detection method for highway volume data. *Physica A: Statistical Mechanics and Its Applications*, *444*, 722–731. https://doi.org/10.1016/j.physa.2015.10.073

Daubechies, I. (1992). Ten Lectures of Wavelets. *Springer-Verlag*.

Daubechies, I. (2004). An iterative thresholding algorithm for linear inverse problems with a sparsity constraint. *Wiley*, *2*, 1413–1457.

Dogangun, I., & Unal, G. (2019). Multifractal behavior in precious metals: Wavelet coherency and forecasting by varima and v-farima models. *Annals of Financial Economics*, *14*(2), 1–12. https://doi.org/10.1142/S2010495219500064

Drod, S., Kwapień, J., Oświecimka, P., & Rak, R. (2009). Quantitative features of multifractal subtleties in time series. *Epl*, *88*(6), 1–6. https://doi.org/10.1209/0295-5075/88/60003

Edwards, F. R., & Caglayan, M. O. (2001). Hedge fund and commodity fund investments in bull and bear markets. *Journal of Portfolio Management*, *27*(4), 97.

Epps, T. W. (1979). Comovements in Stock Prices in the Very Short Run. *Journal of the American Statistical Association*, *74*(366a), 291–298.

Gao, X. L., Shao, Y. H., Yang, Y. H., & Zhou, W. X. (2022). Do the global grain spot markets exhibit multifractal nature? *Chaos, Solitons and Fractals*, *164*(1), 112663. https://doi.org/10.1016/j.chaos.2022.112663

Gencay, R. (2002). *An Introduction to Wavelet and Other Filtering Methods in Finance and Economics*. Elsevier Inc. https://doi.org/https://doi.org/10.1016/B978-0-12-279670-8.X5000-9

Ghazani, M. M., & Khosravi, R. (2020). Multifractal detrended cross-correlation analysis on benchmark cryptocurrencies and crude oil prices. *Physica A*, *560*, 125172. https://doi.org/10.1016/j.physa.2020.125172

Govindan, R. B., Vjushin, D., Brenner, S., Bunde, A., Havlin, S., & Schellnhuber, H. J. (2001). Long-range correlations and trends in global climate models: Comparison with real data. *Physica A: Statistical Mechanics and Its Applications*, *294*(1–2), 239–248. https://doi.org/10.1016/S0378-4371(01)00110-8

Granger, C. . W. . J. . (1969). Investigating Causal Relations by Econometric Models and Cross-spectral Methods. *Econometrica*, *37*(3), 424–438.

Grasseau, M. H. A. A. G. (1988). Wavelet Transform of Multifractals. *Physical Review Letters*, *61*(20).

Grech, D., & Pamuła, G. (2008). The local Hurst exponent of the financial time series in the vicinity of crashes on the Polish stock exchange market. *Physica A: Statistical Mechanics and Its Applications*, *387*(16–17), 4299–4308. https://doi.org/10.1016/J.PHYSA.2008.02.007

Grinsted, A., Moore, J. C., & Jevrejeva, S. (2004). Application of the cross wavelet transform and wavelet coherence to geophysical time series. *Nonlinear Processes in Geophysics*, *11*(5/6), 561–566.

Gu, G. F., & Zhou, W. X. (2006). Detrended fluctuation analysis for fractals and multifractals in higher dimensions. *Physical Review E - Statistical, Nonlinear, and Soft Matter Physics*, *74*(6), 1–7. https://doi.org/10.1103/PhysRevE.74.061104

Gu, G. F., & Zhou, W. X. (2010). Detrending moving average algorithm for multifractals. *Physical Review E - Statistical, Nonlinear, and Soft Matter Physics*, *82*(1), 1–12. https://doi.org/10.1103/PhysRevE.82.011136

Gülerce, M., & Ünal, G. (2016). Using wavelet analysis to uncover the co-movement behavior of multiple energy commodity prices. *International Journal of Wavelets, Multiresolution and Information Processing*, *14*(06), 1650047. https://doi.org/10.1142/S0219691316500478

Hillier, D., Draper, P., Faff, R., Financial, S., Journal, A., Apr, M., Apr, N. M., Taylor, P., Hillier, D., Draper, P., & Faff, R. (2006). Do Precious Metals Shine ? An Investment Perspective. *Financial Analysts Journal*, *62*(2), 98–106.

Holschneider, M. (1988). On the wavelet transformation of fractal objects. *Journal of Statistical Physics*, *50*(5–6), 963–993. https://doi.org/10.1007/BF01019149

Ihlen, E. A. F. (2012). Introduction to multifractal detrended fluctuation analysis in Matlab. *Frontiers in Physiology*, *3 JUN*(June), 1–18. https://doi.org/10.3389/fphys.2012.00141

Jiang, Z. Q., Gao, X. L., Zhou, W. X., & Stanley, H. E. (2017). Multifractal cross wavelet analysis. *Fractals*, *25*(6). https://doi.org/10.1142/S0218348X17500542

Jiang, Z. Q., Xie, W. J., Zhou, W. X., & Sornette, D. (2019). Multifractal analysis of financial markets: A review. *Reports on Progress in Physics*, *82*(12).

https://doi.org/10.1088/1361-6633/ab42fb

Jiang, Z. Q., Yang, Y. H., Wang, G. J., & Zhou, W. X. (2017). Joint multifractal analysis based on wavelet leaders. *Frontiers of Physics*, *12*(6), 1–11. https://doi.org/10.1007/s11467-017-0674-x

Jiang, Z. Q., & Zhou, W. X. (2011). Multifractal detrending moving-average cross-correlation analysis. *Physical Review E - Statistical, Nonlinear, and Soft Matter Physics*, *84*(1), 1–15. https://doi.org/10.1103/PhysRevE.84.016106

Kantelhardt, J. W., Zschiegner, S. A., Koscielny-Bunde, E., Havlin, S., Bunde, A., & Stanley, H. E. (2002). Multifractal detrended fluctuation analysis of nonstationary time series. *Physica A: Statistical Mechanics and Its Applications*, *316*(1–4), 87–114. https://doi.org/10.1016/S0378-4371(02)01383-3

Kim, H., Oh, G., & Kim, S. (2011). Multifractal analysis of the Korean agricultural market. *Physica A: Statistical Mechanics and Its Applications*, *390*(23–24), 4286–4292. https://doi.org/10.1016/j.physa.2011.06.046

Kristoufek, L. (2011). Multifractal height cross-correlation analysis: A new method for analyzing long-range cross-correlations. *Epl*, *95*(6). https://doi.org/10.1209/0295-5075/95/68001

Lin, M., Wang, G. J., Xie, C., & Stanley, H. E. (2018). Cross-correlations and influence in world gold markets. *Physica A: Statistical Mechanics and Its Applications*, *490*, 504–512. https://doi.org/10.1016/j.physa.2017.08.045

Lu, X., Tian, J., Zhou, Y., & Li, Z. (2013). Multifractal detrended fluctuation analysis of the Chinese stock index futures market. *Physica A: Statistical Mechanics and Its Applications*, *392*(6), 1452–1458. https://doi.org/10.1016/j.physa.2012.11.037

Lütkepohl, H. (2004). Forecasting with VARMA Models. *EUI Working Paper ECO*, *25*.

Mallat, S. (2008). *A Wavelet Tour of Signal Processing The Sparse Way* (3rd Editio). Elsevier.

Oral, E., & Unal, G. (2017a). Co-movement of precious metals and forecasting using scale by scale wavelet transform. *International Journal of Financial Engineering*, *4*(1). https://doi.org/10.1142/S2424786317500074

Oral, E., & Unal, G. (2017b). Dynamic correlation of Eastern and Western markets and forecasting: Scale-by-scale wavelet-based approach. *International Journal of Financial Engineering*, *04*(04), 1750040. https://doi.org/10.1142/S2424786317500402

Oral, E., & Unal, G. (2019). Modeling and forecasting time series of precious metals : a new approach to multifractal data. *Financial Innovation*, *5*(22).

Oświęcimka, P., Drożdż, S., Frasca, M., Gębarowski, R., Yoshimura, N., Zunino, L., & Minati, L. (2020). Wavelet-based discrimination of isolated singularities masquerading as multifractals in detrended fluctuation analyses. *Nonlinear Dynamics*, *100*(2), 1689–1704. https://doi.org/10.1007/s11071-020-05581-y

Oygur, T., & Unal, G. (2017). Evidence of Large Fluctuations of Stock Return and Financial Crises from Turkey: Using Wavelet Coherency and Varma Modeling to Forecast Stock Return. *Fluctuation and Noise Letters*, *16*(2), 1–28. https://doi.org/10.1142/S0219477517500201

P.J. Webster, C. T. (1999). Interdecadal Changes in the ENSO – Monsoon System. *Journal of Climate*, *12*, 2679–2690.

Pal, M., Satish, B., Srinivas, K., Rao, P. M., & Manimaran, P. (2015). Multifractal detrended cross-correlation analysis of coding and non-coding DNA sequences through chaos-game representation. *Physica A*, *436*, 596–603. https://doi.org/10.1016/j.physa.2015.05.018

Peng, C.-K., Buldyrev, S. V., Goldberger, A. L., Havlin, S., Sciortino, F., Simons, M., & Stanley, H. E. (1992). Long-range correlations in nucleotide sequence. *Nature*, *359*, 710–713. file:///C:/Users/ASUS/Desktop/Rujukan PhD/p21/xiong1993.pdf

Peng, C.-K., Buldyrev, S. V., Havlin, S., Simons, M., Stanley, H. E., & Goldberger, A. L. (1994). Mosaic organization of DNA nucleotides. *Science*, *42*(2), 1685–1685.

Podobnik, B., Grosse, I., Horvatić, D., Ilic, S., Ivanov, P. C., & Stanley, H. E. (2009). Quantifying cross-correlations using local and global detrending approaches. *European Physical Journal B*, *71*(2), 243–250. https://doi.org/10.1140/epjb/e2009-00310-5

Podobnik, B., Horvatic, D., Petersen, A. M., & Stanley, H. E. (2009). Cross-correlations between volume change and price change. *Proceedings of the National Academy of Sciences of the United States of America*, *106*(52), 22079–22084. https://doi.org/10.1073/pnas.0911983106

Podobnik, B., & Stanley, H. E. (2008). Detrended cross-correlation analysis: A new method for analyzing two nonstationary time series. *Physical Review Letters*, *100*(8), 1–4. https://doi.org/10.1103/PhysRevLett.100.084102

S.Tsay, R. (2013). Multivariate Time Series Analysis With R and Financial Applications. *Wiley Senes in Probability and Statistics*.

Sensoy, A. (2013). Dynamic relationship between precious metals. *Resources Policy*, *38*(4), 504–511. https://doi.org/10.1016/j.resourpol.2013.08.004

The MathWorks, I. (2022). *Continuous and Discrete Wavelet Transforms*. https://www.mathworks.com/help/wavelet/gs/continuous-and-discrete-wavelet-transforms.html

Torrence, C., & Compo, G. P. (1998). A Practical Guide to Wavelet Analysis. *Bulletin of the American Meteorological Society*, *79*(1), 61–78.

Vacha, J. B. E. K. L. (2013). Gold, Oil, and Stocks. *ArXiv Working Paper*.

Wang, G. J., & Xie, C. (2013). Cross-correlations between the CSI 300 spot and futures markets. *Nonlinear Dynamics*, *73*(3), 1687–1696. https://doi.org/10.1007/s11071-013-0895-7

Wang, G. J., Xie, C., Chen, S., & Han, F. (2014). Cross-correlations between energy and emissions markets: New evidence from fractal and multifractal analysis. *Mathematical Problems in Engineering*, *2014*. https://doi.org/10.1155/2014/197069

Wang, G. J., Xie, C., Lin, M., & Stanley, H. E. (2017). Stock market contagion during the global financial crisis: A multiscale approach. *Finance Research Letters*, *22*, 163–168. https://doi.org/10.1016/j.frl.2016.12.025

Wang, J., Shang, P., & Ge, W. (2012). Multifractal cross-correlation analysis based on statistical moments. *Fractals*, *20*(3–4), 271–279. https://doi.org/10.1142/S0218348X12500259

Wang, Y., Wu, C., & Pan, Z. (2011). Multifractal detrending moving average analysis on the US Dollar exchange rates. *Physica A: Statistical Mechanics and Its Applications*, *390*(20), 3512–3523. https://doi.org/10.1016/j.physa.2011.05.023

Weber, R. O., & Talkner, P. (2001). Spectra and correlations of climate data from days to decades. *Journal of Geophysical Research Atmospheres*, *106*(D17), 20131–20144.

https://doi.org/10.1029/2001JD000548

Xie, C., Zhou, Y., Wang, G., & Yan, X. (2017). Analyzing the Cross-Correlation between Onshore and Offshore RMB Exchange Rates Based on Multifractal Detrended Cross-Correlation Analysis (MF-DCCA). *Fluctuation and Noise Letters*, *16*(1). https://doi.org/10.1142/S0219477517500043

Xie, W. J., Jiang, Z. Q., Gu, G. F., Xiong, X., & Zhou, W. X. (2015). Joint multifractal analysis based on the partition function approach: Analytical analysis, numerical simulation and empirical application. *New Journal of Physics*, *17*(10). https://doi.org/10.1088/1367-2630/17/10/103020

Yilmaz, A., & Unal, G. (2016). Co-movement analysis of Asian stock markets against FTSE100 and S&P 500: Wavelet-based approach. *International Journal of Financial Engineering*, *03*(04), 1650033. https://doi.org/10.1142/S242478631650033X

Ying, Y., Xin-tian, Z., & Xiu, J. (2009). Measuring multifractality of stock price fluctuation using multifractal detrended fluctuation analysis. *Physica A*, *388*(11), 2189–2197. https://doi.org/10.1016/j.physa.2009.02.026

Zebende, G. F. (2011). DCCA cross-correlation coefficient: Quantifying level of cross-correlation. *Physica A: Statistical Mechanics and Its Applications*, *390*(4), 614–618. https://doi.org/10.1016/j.physa.2010.10.022

Zhou, W. X. (2008). Multifractal detrended cross-correlation analysis for two nonstationary signals. *Physical Review E - Statistical, Nonlinear, and Soft Matter Physics*, *77*(6), 2–5. https://doi.org/10.1103/PhysRevE.77.066211

Zhou, W. X. (2009). The components of empirical multifractality in financial returns. *Europhysics Letters*, *88*(2), 1–7. https://doi.org/10.1209/0295-5075/88/28004

Zhou, W. X. (2012). Finite-size effect and the components of multifractality in financial volatility. *Chaos, Solitons and Fractals*, *45*(2), 147–155. https://doi.org/10.1016/j.chaos.2011.11.004

Appendix A. List of Abbreviations

- V-FARIMA - Vector Autoregressive Fractionally Integrated Moving Average
- VARIMA – Vector Autoregressive Integrated Moving Average
- VAR – Vector Autoregressive
- VARMA - Vector Autoregressive Moving Average
- ARMA - Autoregressive Moving Average
- ARIMA – Autoregressive Integrated Moving Average
- MF-DFA – Multifractal Detrending Fluctuations Analysis
- H – Hölder Exponent
- DWT – Discrete Wavelet Transform
- CWT – Continuous Wavelet Transform
- WPT – Wavelet Packet Transform
- FWT – Fast Wavelet Transform
- XWT – Cross Wavelet Transform
- PDS – Phase-Difference Spectrum
- COI – Cone of Influence
- XAU - Spot Gold
- XPT – Spot Platinum
- CUSUM – Cumulative Sum
- WTC – Wavelet Transform Coherence
- MF-X-DMA – Multifractal Cross-Correlation Detrened Moving Average
- MF-DFA – Multifractal Detrended Fluctuation Analysis
- MF-X-PF – Multifractal Analysis Based On Partition Function

- MFSMXA – Multifractal Cross-Correlation Analysis Based On Statistical Moments
- MF-HXA – Multifractal Height Cross-Correlation Analysis
- MF-X-DFA – Multifractal Cross-Correlation Detrened Fluctuation Analysis
- DCCA – Detrended Cross-Correlation Analysis
- MF-DMA – Multifractal Detrended Moving Average
- DMA – Detrended Moving Average
- MF-CCA – Multifractal Cross-Correlation Analysis
- MFDPXA – Multifractal Detrended Partial Cross-Correlation Analysis
- MF-PX-DFA – Multifractal Partial Cross-Correlation Detrended Fluctuation Analysis
- MF-PX-DMA – Multifractal Partial Cross-Correlation Detrended Moving Average
- FA – Fluctuation Analysis
- DFA – Detrended Fluctuation Analysis
- MF-DCCA – Multifractal Detrended Cross-Correlation Analysis
- OTC – Over the Counter
- WTMM – Wavelet Transform Modulus Maxima

Appendix B. List of Symbols

- $Y(i)$ - integrated signal profile
- $F_q(s)$ - The function of q^th order fluctuation
- h(q)- Generalized Hurst Exponent
- H- Hurst Exponent
- v-Segment
- $\varphi(\eta)$ – Morlet Wavelet
- $Wx(\tau,s)$ - Continuous Wavelet Transform
- $W_n^x(s)$ – Wavelet Transform
- $|Wxy(u,s)|$ - Cross Wavelet Power
- $R_s^2(u,s)$ – squared wavelet coherence coefficient
- ψ_{xy}(u, s) – Phase difference
- $A_0 y_t$- Multivariate Autoregressive Moving Average
- $\psi_0(n)$- Wavelet Function
- $\tilde{Z}$(t) – Moving Average Function
- $\varepsilon(i)$- Cross-Correlation residual Series
- $F(s,v)$- Cross-Correlation Variance
- $F_{xy}(q,s)$ – Fluctuation Function
- ρ_{DCCA} – Detrended Cross-Correlation Coefficient
- $\tau_{xy}(q)$ – Renyi Exponent
- $f_{xy}(\alpha)$ – Multifractal Spectrum